results in a large number of unnecessary biopsies [2]. Several modifications of PSA-related indices such as PSA isoforms and volume-referenced PSA have been investigated to improve the specificity of PSA in detecting prostate cancer [3–5]. Free/total PSA ratio (f/t PSA) is widely used in clinical practice to differentiate prostate cancer from BPH in men with grey zone PSA levels, but this does not have sufficient specificity to reduce unnecessary biopsies. Thus, more accurate and reliable assessments are needed to select candidates for prostate biopsy.

Bussemakers et al. [6]reported that prostate cancer gene 3 (PCA3) produces an untranslated, prostate-specific messenger RNA (mRNA) that is highly overexpressed in prostate cancer tissue compared with its level in normal or benign tissue. Several studies have shown that PCA3 urine assay is superior to serum PSA level or various PSA isoforms for predicting prostate cancer in European and US men, and it could be used as a diagnostic tool to select biopsy candidates [7–10]. We have previously demonstrated the high specificity of PCA3 urine assay in detecting prostate cancer in a limited number of Japanese men at a single institution [11]. In the present multicentre study, we investigated the diagnostic performance of this assay in a large cohort of Japanese men.

Methods

The study protocol was approved by the institutional review boards and all men provided written informed consent before enrolment in the present study. A total of 647 men with elevated serum PSA levels and/or an abnormal DRE were enrolled. They underwent systematic extended prostate biopsy (≥8 cores) at one of four Japanese institutions (Kyoto Prefectural University of Medicine, Japanese Red Cross Medical Centre, University of Tsukuba and Kinki University) from 2009 to May 2011. The ethnic origin of all patients was Asian. Among the 647 cases, 158 had a previous negative biopsy. The exclusion criteria were as follows: previous history of prostate cancer, taking medication known to affect serum PSA levels, UTIs, and history of invasive treatment for BPH. The first voided urine sample was collected after a DRE, and the urine specimen was examined using a PROGENSA PCA3 assay according to a previously described method [11]. The PCA3 score was determined using PCA3 mRNA copy divided by PSA mRNA copy. The f/t PSA was measured in men with PSA 4–10 ng/mL. Prostate volume (PV) was measured using ultrasonography and PSA density (PSAD) was calculated by dividing PSA by PV. Clinical and pathological outcomes such as clinical stage, Gleason score and percentage of positive cores (% positive cores) in men diagnosed with prostate cancer were correlated with PCA3 score. The % positive cores was calculated as the number of positive cores divided by the number of cores taken, and patients were divided into two groups according to % positive cores (≤33% or >33%). Indolent cancer was defined, according to the Epstein criteria, as clinical stage T1c, PSAD < 0.15, Gleason score ≤ 6, and <3 positive cores on a six-core biopsy, which was replaced by % positive cores ≤ 33 with biopsy sampling of more than six cores [12]. The Mann–Whitney test was used to compare continuous variables among the groups. The chi-squared test was used to assess nominal variables. Bivariate analysis (Pearson's correlation coefficient '*r*') was used to test the linearity of relationships among the variables. Areas under the receiver–operator curves (AUCs) were compared. Multiple stepwise logistic regression analysis was used to determine the significant predictors of positive biopsy among variables such as repeated biopsy or not, PSA, PV, PSAD and PCA3 score. These statistical analyses were performed using commercially available software (SPSS version 12.0, Chicago, IL, USA). A P value of <0.05 was considered to indicate statistical significance.

Results

Among 647 urine samples, 633 were successfully analysed (the informative rate was 98%). The median (range) age, PSA level and number of biopsy cores taken were 69 (42–89) years, 7.6 (1.4–1908) ng/mL and 12 (6–59), respectively. Two patients had a six-core biopsy. There was no relationship between the PCA3 score and serum PSA level ($r = 0.049$, nonsignificant). Prostate biopsy was positive for prostate cancer in 264 men (41.7%). The characteristics of the men with positive and negative biopsies are shown in Table 1. The median PCA3 score in men with prostate cancer was significantly higher than that in those without prostate cancer (49 vs 18, $P < 0.001$). The positive rate of biopsy is shown in Table 2. We excluded all men who had a PSA level > 50 ng/mL and men who had initial biopsy with PSA of 20–50 ng/mL from further analyses because of the high yield of positive biopsy results; thus, the remaining 578 men were entered for analysis. The percentage of men with positive biopsy increased with increasing PCA3 score (Fig. 1). In men with a PCA3 score < 20, 16.0% (38/237) had a positive biopsy. When the PCA3 score was ≥50, the percentage of patients with a positive biopsy was 60.6% (106/175). Sensitivity, specificity, positive and negative predictive values of PCA3 scores at different PSA thresholds are shown in Table 3. Using a PCA3 threshold of 35, the sensitivity, specificity and diagnostic accuracy were 66.5, 71.6 and 69.7%, respectively. The AUCs of PSA, PV, PSAD and PCA3 score in 561 available men were 0.583, 0.706, 0.712 and 0.748, respectively. There was a significant difference in AUC between PSA and PCA3 score ($P < 0.001$), but not between PSAD and PCA3 score. Thirty-eight out of 408 men with PSA of 4–10 ng/mL had missing values of either PV or f/t PSA. In 370 available men

Table 1 Characteristics of patients with negative and positive biopsy results.

Characteristic	Negative biopsy, $n = 369$	Positive biopsy, $n = 264$	P
	Median (range)	Median (range)	
Age, years	67 (42–89)	71 (49–88)	<0.001
PSA, ng/mL	7.0 (1.4–42.6)	9.0 (2.2–1908)	<0.001
PV*, mL	38 (9.4–130)	29.1 (8.2–109)	<0.001
PSAD	0.18 (0.03–1.38)	0.36 (0.07–80.84)	<0.001
No. of cores	12 (6–59)	12 (6–40)	N.S.
PCA3 score	18 (0–381)	49 (1–288)	<0.001

**22 cases not available. N.S., nonsignificant.*

Table 2 Positive rate of prostate cancer by serum PSA range.

PSA,ng/mL	Total		Initial biopsy		Repeat biopsy	
	n	Prostate cancer (%)	n	Prostate cancer (%)	n	Prostate cancer (%)
≤4	22	5 (22.7)	21	5 (23.8)	1	0 (0)
4–10	408	140 (34.3)	316	120 (38.0)	92	20 (21.7)
10–20	131	64 (48.8)	85	44 (51.8)	46	20 (43.5)
20–50	46	29 (63.0)	29	23 (79.3)	17	6 (37.9)
>50	26	26 (100)	25	25 (100)	1	1 (100)
Total	633	264 (41.7)	476	217 (45.6)	157	47 (29.9)

Fig. 1 Percentage of men with positive biopsy by PCA3 score range ($N = 578$).

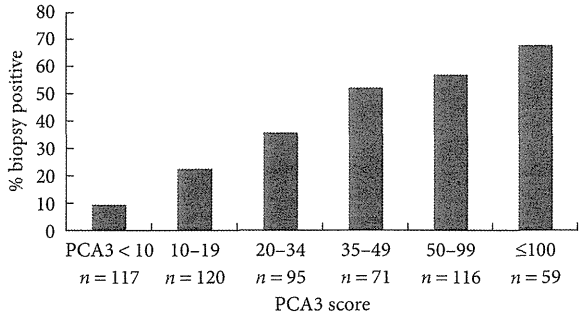

with PSA of 4–10 ng/mL, the AUCs of PSA, f/t PSA, PV, PSAD and PCA3 score were 0.557, 0.647, 0.686, 0.692 and 0.742, respectively. There was a significant difference in AUC between f/t PSA and PCA3 score ($P < 0.05$), but not between PSAD and PCA3 score (Fig. 2). On univariate regression analysis, all variables had a significant association with biopsy outcome. Multivariate logistic regression analysis showed that PCA3 score ($P < 0.001$), PSAD ($P < 0.001$), PV ($P < 0.01$) and repeated biopsy ($P < 0.01$) were independent factors predicting biopsy outcome (Table 4). Totals of 21.1% (32/152), 22.9% (27/118) and 51.5% (150/291) of patients had a positive biopsy in patients with PSAD < 0.15, 0.15–0.2 and ≥0.2, respectively. The percentage of men with positive biopsy according to the combination of PSAD and PCA3 score is shown in Fig. 3. The percentage of patients with a positive biopsy increased with higher PCA3 scores in subgroups based on PSAD. Only three (4.1%) out of 72 cases with PSAD < 0.15 and PCA3 score < 20 had prostate cancer. A total of 43% had a positive biopsy in men with PSAD < 0.15 and PCA3 score ≥50. In 264 men diagnosed with prostate cancer, a total of 72, 103 and 89 cases had Gleason scores ≤ 6, 7, and ≥8, respectively. Median (range) PCA3 scores in men with Gleason scores ≤ 6, 7 and ≥8 were 45 (4–280), 51 (4–288), and 45 (1–250), respectively. There was no significant difference in PCA3 score among these three groups. A total of 88, 133, 35 and eight patients had clinical stage T1c, T2, T3, and T4, respectively. Median (range) PCA3 scores in men with clinical stage T1c, T2, T3, and T4 were 44 (6–242), 55 (4–280), 49 (1–288), and 51 (15–123), respectively. There was no significant difference in PCA3 score among the four categorical groups of clinical stage. There was a significant association between PCA3 score and % positive cores ($r = 0.166$, $P < 0.01$). Data on % positive cores was not available in two patients. A total of 164 and 98 cases had % positive cores ≤ 33, and >33, respectively. A total of 12 and 248 cases had indolent cancer and significant cancer, respectively. There was no significant difference in PCA3 score between % positive cores ≤ 33 and >33 (median PCA3 score 47 vs 58), or between indolent cancer and significant cancer (median PCA3 score 39 vs 49).

Discussion

In the present study, we investigated the ability of a PCA3 urine assay to predict the prostate biopsy outcome in a

Table 3 Sensitivity, specificity, positive and negative predictive values at different PCA3 score thresholds.

PCA3 score	Sensitivity	Specificity	Positive predictive value	Negative predictive value
10	94.9	29.2	44.3	90.6
20	82.3	54.8	51.9	84.0
35	66.5	71.6	58.1	78.3
50	49.3	81.0	60.6	73.0
100	18.6	94.8	67.8	66.3

Fig. 2 A, Receiver – operator curve (ROC) analysis to predict positive biopsy results (n = 561), PSA: 0.583, PV: 0.706, PSAD: 0.712, PCA3 score: 0.748. PSA vs. PCA3 score: $P < 0.001$, PV, PSAD vs. PCA3 score N.S. **B**, ROC analysis to predict positive biopsy result in patients with PSA between 4 and 10 ng/mL (n = 370), PSA: 0.557, f/t PSA: 0.647, PV: 0.686, PSAD: 0.692, PCA3 score: 0.742, PSA vs PCA3 score $P < 0.001$, f/t PSA vs. PCA3 score: $P < 0.05$, PV, PSAD vs. PCA3 score N.S.

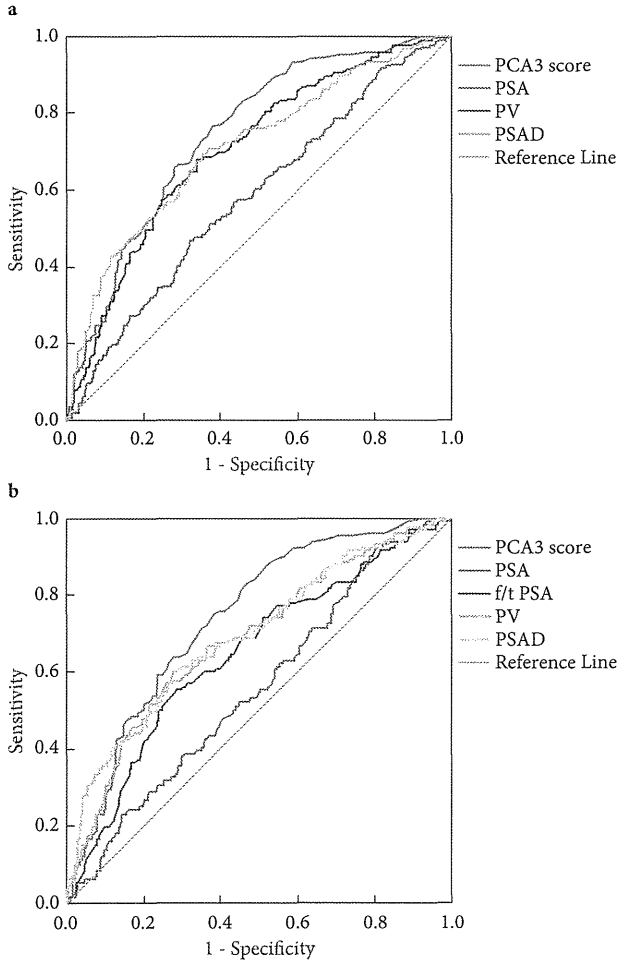

large cohort of patients from four major institutions in Japan. We found the highly informative specimen rate of 98% using a PROGENSA PCA3 assay, which verified the results of multiple studies [7–11]. We observed an increasing incidence of prostate cancer in men with a higher PCA3 score. The diagnostic performance of PCA3 urine assay for prostate cancer was excellent, with an AUC of 0.748 in Japan, compared with other reports in North America and Europe ranging from 0.66 to 0.69 [8–10,13]. Adam et al. [14] reported that the AUC of PCA3 was 0.7054 in a South African setting consisting of 68% black men. At a PCA3 threshold of 35, which is considered to be a better balanced value between sensitivity and specificity, the specificity of the PCA3 score was 71.6% in Japanese men, compared with 72–76% in North American and European men and 50% in South African men. These results showed that the diagnostic performance of PCA3 assay in Japan was similar to that reported in different regions and ethnic groups.

Free/total PSA ratio is widely used to stratify the risk of prostate cancer in men with PSA 4–10 ng/mL, and a lower f/t PSA is more likely to be found in association with prostate cancer [4]. In the present study, we found that the diagnostic performance of PCA3 score surpassed that of f/t PSA in men with PSA 4–10 ng/mL. The AUC of the PCA3 score was highest among the variables analysed and it was significantly higher than that of f/t PSA (0.742 vs 0.647; $P < 0.05$). In the placebo arm of the Reduction by Dutasteride of Prostate Cancer Events (REDUCE) trial, 1140 men who had a negative baseline biopsy received a PCA3 score before repeat biopsy at 2 years [15]. In its largest repeat biopsy study to date, the AUCs of PCA3 score, PSA, and f/t PSA were 0.693, 0.612 and 0.637, respectively. A significant difference was found between PCA3 score and PSA, but the difference between PCA3 score and f/t PSA did not reach statistical significance ($P = 0.065$). In 463 European men with repeat biopsy, the AUC of PCA3 score was higher than that of f/t PSA (0.658 vs 0.578); however, the difference in AUCs between PCA3 score and f/t PSA did not reach statistical significance either [10]. We confirmed that PCA3 score was significantly superior to f/t PSA and PSA in predicting biopsy outcome in Japanese men with grey zone PSA levels.

Table 4 Univariable and multivariable logistic regression analysis for positive biopsy.

Variable	Univariable			Multivariable		
	OR	95% CI	P	OR	95% CI	P
Repeat biopsy	0.626	0.422–0.930	<0.05	0.521	0.319–0.849	<0.01
PSA	1.058	1.022–1.096	<0.01			N.S.
PV	0.955	0.942–0.968	<0.001	0.978	0.963–0.992	<0.01
PSAD	60.885	18.671–198.536	<0.001	18.883	4.805–74.208	<0.001.
PCA3 score	1.017	1.013–1.022	<0.001	1.015	1.010–1.020	<0.001

Fig. 3 Percentage of men with positive biopsy by combination of PCA3 score range and PSAD range.

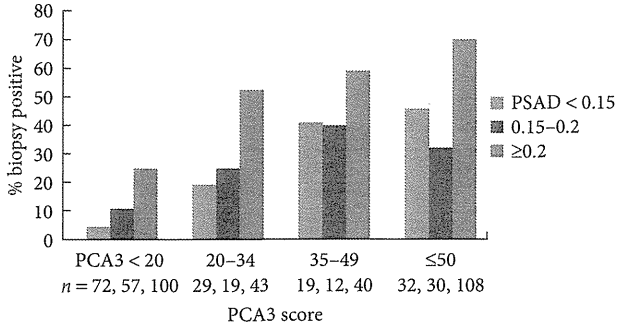

Multivariable logistic regression showed that PCA3 score ($P < 0.001$), PSAD ($P < 0.001$), PV ($P < 0.01$) and repeated biopsy ($P < 0.01$) were independent predictors of positive biopsy in the present study. Several studies showed that PCA3 score was significantly cooperating with PSA and PV for predicting prostate cancer [9,10,13]. PSA correlates with PV in men without prostate cancer; thus, PSAD (PSA divided by PV) was used for more accurate assessment to improve the specificity in diagnosis of prostate cancer; however, the commonly used PSAD threshold of 0.15 could not detect > 40% of cancers, resulting in limited usefulness in a routine clinical setting [5]. In the present study, 21.1% of men with PSAD < 0.15 had a positive biopsy. Thus, when a PSAD threshold value of 0.15 was applied in our population, a considerable number of prostate cancer cases were missed. When the PCA3 score was combined with PSAD, we observed that the rate of positive biopsy increased, even in the subgroup of men with PSAD < 0.15 (Fig. 3). When the PCA3 score was <20 in men with PSAD < 0.15, only three (4.1%) out of 72 men had prostate cancer. By contrast, 43% of men with PCA3 score ≥50 and PSAD < 0.15 had a positive biopsy. The combination of PSAD and PCA3 score stratifies the risk of prostate cancer and predicts a low risk of prostate cancer, suggesting that these men could avoid unnecessary biopsy. It is notable that these three patients with cancer (PSAD < 0.15 and PCA3 score <20) had significant cancer with % positive cores of ≤33 and Gleason score > 6 as biopsy pathological features.

Several studies have shown the significant relationship between PCA3 score and tumour volume in prostatectomy specimens and the ability of PCA3 score to discriminate low-volume/low-grade cancer with the aim of selecting patients who are candidates for active surveillance [16,17]. Ploussard et al. [17]reported that a high PCA3 score of >25 was an important predictor of large tumour volume with an odds ratio of 5.4 ($P = 0.1$) and significant cancer with an odds ratio of 12.7 ($P = 0.003$). In the present study, we found a significant relationship between PCA3 score and % positive cores; however, there was no difference in PCA3 score between % positive ≤ 33 and >33, or among subgroups by Gleason score and clinical stage. Further investigation of the correlation between PCA3 score and pathological outcomes on prostatectomy specimens will be needed in Japan.

In the present cohort, men with a wide range of PSA levels were enrolled. A PCA3 urine assay would be irrelevant in men with a high PSA level (the positive rate of prostate cancer was 100% in men with PSA > 50 ng/mL, and 79.3% in men with PSA 20–50 ng/mL at initial biopsy); thus, these were excluded from the analysis for prediction of biopsy outcome. Furthermore, not all men received prostate volume measurement because this was a multi-institutional study. These features might have influenced the results.

In conclusion, this Japanese multicentre study shows that the PCA3 urine assay could improve the prediction of prostate cancer and may help in selecting men who might benefit from prostate biopsy. The percentage of patients with positive biopsy increased with higher PCA3 scores. PCA3 score was superior to f/t PSA for predicting prostate cancer in patients with PSA 4–10 ng/mL. A combination of PSAD and PCA3 score may be useful for selecting patients who could avoid an unnecessary biopsy.

Acknowledgements

We wish to thank Fujirebio Inc. for their technical assistance.

Conflict of Interest

None declared.

References

1 **Catalona WJ, Smith DS, Raliff TL et al.** Measurement of prostate –specific antigen in serum as a screening test for prostate cancer. *N Engl J Med* 1991; 324: 1156–61

2 **Thompson IM, Pauler DK, Goodman PJ et al.** Prevallence of prostate cancer among men with a prostate-specific antigen level< or =4.0 ng per milliliter. *N Engl J Med* 2004; 350: 2239–46

3 **Babaian RJ, Kojima M, Ramirez EI et al.** Comparison analysis of prostate specific antigen and its indexes in the detection of prostate cancer. *J Urol* 1996; 156: 432–7

4 **Catalona WJ, Partin AW, Slawin KM et al.** Use of the percentage of free prostate-specific antigen to enhance differentiation of prostate cancer form benign prostatic disease: a prospective multicenter clinical trial. *JAMA* 1998; 279: 1542–7

5 **Catalona WJ, Southwick PC, Slawin KW et al.** Comparison of percent free PSA, PSA density and age specific PSA cutoffs for prostate cancer detection and staging. *Urology* 2000; 56: 255–60

6 **Bussemakers MJG, Bokhoven AV, Verhaegh GW et al.** DD3: a new prostate-specific gene, highly overexpressed in prostate cancer. *Cancer Res* 1999; 59: 5975–9

7 **Groskopf J, Aubin SMJ, Deras IL et al.** APTIMA PCA3 molecular urine test: development of a method to aid in the diagnosis of prostate cancer. *Clin Chem* 2006; 52: 1089–95

8 **Marks LS, Fradet Y, Deras IL et al.** PCA3 molecular urine assay for prostate cancer in men undergoing repeat biopsy. *Urology* 2007; 69: 532–5

9 **Deras IL, Aubin SM, Blasé A et al.** PCA: a molecular urine assay for predicting prostate biopsy outcome. *J Urol* 2008; 179: 1587–92

10 **Haese A, Taille A, Poppel H et al.** Clinical utility of the PCA3 urine assay in European men scheduled for repeated biopsy. *Eur Urol* 2008; 54: 1081–8

11 **Ochiai A, Okihara K, Kamoi K et al.** Prostate cancer gene 3 urine assay for prostate cancer in Japanese men undergoing prostate biopsy. *Int J Urol* 2011; 18: 200–5

12 **Epstein JI, Walsh PC, Carmichael M et al.** Pathologic and clinical findings to predict tumor extent of non palpable (stag T1c) prostate cancer. *JAMA* 1994; 271: 368–74

13 **Chun FK, Taille ADL, Poppel HV et al.** Prostate cacner gene 3 (PCA3): development and internal validation of a novel biopsy nomogram. *Eur Urol* 2009; 56: 659–68

14 **Adam A, Engelbrecht MJ, Bornman MS et al.** The role of the PCA3 assay in predicting prostate biopsy outcome in a South African setting. *BJU Int* 2011; 108: 1728–33

15 **Aubin SMJ, Reid J, Sarno MJ et al.** PCA3 molecular urine test for predicting repeat prostate biopsy outcome in populations at risk: validation in the placebo arm of the Dutasteride REDUCE trial. *J Urol* 2010; 184: 1947–52

16 **Nakanishi H, Groskopf J, Fritsche HA et al.** PCA3 molecular urine assay correlates with prostate tumor volume: implication in selecting candidate for active surveillance. *J Urol* 2008; 179: 1804–10

17 **Ploussard G, Durand X, Xylinas E et al.** Prostate cancer antigen 3 score accurately predicts tumour volume and might help in selecting prostate cancer patients for active surveillance. *Eur Urol* 2011; 59: 422–9

Correspondence: Atsushi Ochiai, Department of Urology, Kyoto Prefectural University of Medicine, 465 Kajiicho, Kawaramachi-Hirokoji, Kamigyoku, Kyoto 602-8566, Japan.

e-mail: chikamika2001@yahoo.co.jp

Abbreviations: PCA3, prostate cancer gene 3; f/t PSA, free/total PSA ratio; mRNA, messenger RNA; PV, prostate volume; PSAD, PSA density; AUC, area under the receiver–operator curve.

Expression and Role of HMGA1 in Renal Cell Carcinoma

Natsuki Takaha,* Yoshihiro Sowa, Ichiro Takeuchi, Fumiya Hongo, Akihiro Kawauchi and Tsuneharu Miki

From the Departments of Translational Cancer Drug Development (NT, TM) and Urology (NT, IT, FH, AK, TM) and Molecular-Targeting Cancer Prevention (YS), Kyoto Prefectural University of Medicine, Kyoto, Japan

Purpose: Although molecular targeted therapy has improved the clinical outcome of metastatic renal cell carcinoma, a complete response is rare and there are various side effects. Identifying novel target molecules is necessary to improve the clinical outcome of metastatic renal cell carcinoma. HMGA1 is over expressed in many types of cancer and it is associated with metastatic potential. It is expressed at low levels or not expressed in normal tissue. We examined HMGA1 expression and function in human renal cell carcinoma.

Materials and Methods: HMGA1 expression in surgical specimen from patients with renal cell carcinoma was examined by immunoblot. HMGA1 expression in 6 human renal cell carcinoma cell lines was examined by immunoblot and immunofluorescence. The molecular effects of siRNA mediated knockdown of HMGA1 were examined in ACHN and Caki-1 cells.

Results: Immunoblot using surgical specimen showed that HMGA1 was not expressed in normal kidney tissue but it was expressed in tumor tissue in 1 of 30 nonmetastatic (3%) and 6 of 18 metastatic (33%) cases ($p = 0.008$). Immunoblot and immunofluorescence revealed significant nuclear expression of HMGA1 in ACHN and Caki-1 cells derived from metastatic sites. HMGA1 knockdown remarkably suppressed colony formation and induced significant apoptosis in ACHN and Caki-1 cells. HMGA1 knockdown significantly inhibited invasion and migration in vitro, and induced anoikis associated with P-Akt down-regulation in ACHN cells.

Conclusions: HMGA1 is a potential target for novel therapeutic modalities for metastatic renal cell carcinoma.

Key Words: apoptosis; carcinoma, renal cell; HMGA1 protein; molecular targeted therapy; anoikis

Abbreviations and Acronyms

HMGA1 = high mobility group protein AT-hook 1

mRCC = metastatic RCC

P-Akt = phosphorylated Akt

poly-HEMA = poly 2-hydroxyethyl methacrylate

RCC = renal cell carcinoma

Submitted for publication September 15, 2011.

Study received institutional review board approval.

* Correspondence: Departments of Translational Cancer Drug Development and Urology, Kyoto Prefectural University of Medicine, Kawaramachi-Hirokoji, Kamigyo-ku, Kyoto 602-8566, Japan (telephone: +81-75-251-5595; FAX: +81-75-251-5598; e-mail: ntakaha@koto.kpu-m.ac.jp).

ALTHOUGH molecular targeted therapy has improved the clinical outcome for patients with mRCC, a complete response is rare and therapy has various adverse effects.[1] Identifying novel target molecules is needed to develop new therapeutic modalities for mRCC. Targeting molecules that have a role in cell growth and survival, and are expressed exclusively in cancer cells but not in normal cells should result in significant antitumor effects with few adverse events.

From this perspective we focused on HMGA1, a nuclear matrix protein with 3 AT-hook domains that bind the minor groove of AT-rich DNA sequences.[2] HMGA1 modulates the activity of many transcription factors by inducing a conformational change in DNA via AT rich DNA sequence binding.[2] HMGA1 also modulates the molecular or cellular function of other molecules, including p53[3] and Rb,[4] via protein-protein interactions. HMGA1 is over expressed in many types of can-

0022-5347/12/1876-2215/0
THE JOURNAL OF UROLOGY®

Vol. 187, 2215-2222, June 2012
Printed in U.S.A.
DOI:10.1016/j.juro.2012.01.069

cer[5] but it is expressed at low levels or not expressed in normal adult tissue.[6] HMGA1 exerts oncogenic activity in vitro[7,8] and in vivo.[9–11] HMGA1 expression is associated with cancer metastatic potential and progression.[5,12–14]

We previously reported that HMGA1 transfection in prostate cancer cells enhanced tumor cell growth and matrix metalloproteinase 2 expression[15] while HMGA1 expression in the TRAMP (transgenic adenocarcinoma of the mouse prostate) model was confined to the later stage when metastatic lesions formed.[16] These findings suggest that HMGA1 is a strong candidate gene with a potential role in prostate cancer progression and metastasis.

Thus, we examined HMGA1 expression in RCC cell lines and RCC tissues, and the role of HMGA1 in RCC with an emphasis on HMGA1 as a target molecule for novel therapeutic modalities for mRCC, including antisense therapy.

MATERIALS AND METHODS

Cell Culture and Reagents

The human cancer cell lines PC-3 (prostate cancer), Caki-1, ACHN, NC65, A498, 786-O and RCC4 (RCC) were maintained in RPMI1640 containing 10% fetal bovine serum, 100 U/ml penicillin and 100 μg/ml streptomycin at 37C in a humidified atmosphere of 5% CO_2. We used the pancaspase inhibitor zVAD-fmk (R & D Systems®) and poly-HEMA (Sigma®).

Immunofluorescence

After fixation in methanol and blocking, cultured cells were incubated with anti-HMGI(Y) antibodies (N19) (dilution 1:100) and then with fluorescein conjugated donkey anti-goat IgG (Santa Cruz Biotechnology, Santa Cruz, California) (dilution 1:200). Samples were observed by fluorescence microscopy (Olympus®).[17]

Protein Preparation

Whole cell lysate was prepared from each cell line in RIPA Lysis Buffer (Santa Cruz Biotechnology) according to manufacturer instructions. Each whole cell lysate was prepared from surgical specimens in sodium dodecyl sulfate buffer, as previously described.[18] The protein concentration was measured using a BCA™ Protein Assay Kit.

Immunoblot

Protein samples were separated in 15% polyacrylamide gel (Bio-Rad®) and transferred to nitrocellulose membranes (GE Healthcare, Little Chalfont, United Kingdom). Primary antibodies against HMGA1 (anti-HMGI [Y] antibodies, N19, Santa Cruz Biotechnology), P-Akt (Ser473) and Akt (Total Akt, Cell Signaling Technology®) were used (dilution 1:200, 1:1,000 and 1:2,000, respectively). Signals corresponding to HMGA1, P-Akt and Total Akt were detected using an enhanced chemiluminescence kit (GE Healthcare). A monoclonal antibody against β-actin (clone AC15, Sigma) (dilution 1:5,000) was used to control sample loading. The β-actin signal was detected with a chemiluminescence kit (GE Healthcare).

Patients

Surgical specimens from 48 patients diagnosed histopathologically with RCC who underwent radical nephrectomy were examined by immunoblot. Correlations between HMGA1 expression and clinicopathological factors were analyzed. The patients included 34 males and 14 females 33 to 83 years old. The histopathological diagnosis included clear cell carcinoma in 36 cases, spindle cell carcinoma in 5, chromophobe cell carcinoma in 3, papillary RCC in 2 and an unclassified subtype in 2. Histological classification and stage data according to the 2002 TNM classification system, 6th edition were T1a in 10 cases, T1b in 11, T2 in 4, T3a in 7, T3b in 13, T4 in 3, N0 in 43, N1 in 2, N2 in 3, M0 in 18, M1 in 30, stages I to IV in 19, 2, 9 and 18, and G1 to G3 in 3, 33 and 9, respectively. Normal and cancerous tissues were collected separately from each surgically removed kidney. Specimens were stored frozen at −80C until used for immunoblot.

This study was done with the approval of our institutional review board. Informed consent was obtained from each patient.

siRNA Mediated Knockdown

Synthetic double strand siRNAs were transfected at a concentration of 200 nM using Oligofectamine™ according to manufacturer instructions. The siRNAs used had the sequence (target sequence, sense strand) scramble (control) siRNA 5′-CAGTCGCGTTTGCGACTGGdTdT-3′ and HMGA1 siRNA 5′-GACCCGGAAAACCACCACAdTdT-3′ (Sigma).[19]

Assays

Colony formation. Two days after siRNA transfection cells were seeded at 150 live cells per well in 6-well plates. Cells were incubated in growth medium for 8 to 10 days. The number of viable colonies per well was counted.

Cell proliferation. Two days after siRNA transfection cells were seeded in replicates of 6 into 96-well plates at 5,000 live cells per well in growth medium. Cell proliferation was estimated using the Cell Counting Kit-8 (WST-8) (Dojindo Laboratories, Kumamoto, Japan) according to manufacturer instructions.

Apoptosis Detection

To detect apoptosis by flow cytometry cells were grown for the indicated duration after siRNA transfection and then treated with 0.1% Triton X-100 containing propidium iodide to stain nuclei or labeled using the FITC Annexin V Apoptosis Detection Kit 1 (BD Pharmingen™). DNA content and annexin V positive cells were measured using a FACSCalibur™ flow cytometer and CellQuest™ software. Apoptosis was evaluated by quantifying the percent of cells with hypodiploid DNA (sub-G1) as an indicator of DNA fragmentation or the percent positively stained with annexin V. For all assays 10,000 cells were counted.

Cell Invasion and Migration Assays

Migration and invasion assays were performed using uncoated and Matrigel™ coated Transwell® inserts according to manufacturer instructions. Two days after siRNA transfection 5×10^4 and 2×10^5 live cells were added to the inserts for migration and invasion assays, respectively. After 24-hour incubation at 37C in a humidified 5%

CO_2 atmosphere cells that had migrated through or invaded the inserts were stained using a Diff-Quik™ staining kit and quantified by determining the total cell number derived from 5 randomly chosen visual fields per membrane at 400× magnification.

Anoikis Evaluation

Anoikis was examined by plating cells on poly-HEMA coated 6-well plates to produce a cell suspension according to a previously reported method[20] with minor modifications. A solution of 30 mg/ml poly-HEMA in 95% ethanol was made and 0.96 ml of this solution was overlaid on 1 well of the 6-well plates. The plates were left to dry in a sterile culture hood at room temperature overnight. Before use the wells were rinsed twice with phosphate buffered saline (–) and once with culture medium. Two days after siRNA transfection cells were plated at 2.0×10^5 live cells in each poly-HEMA coated well (nonadherent condition) or in each uncoated well (adherent condition) and incubated for 24 hours at 37C in a humidified 5% CO_2 atmosphere. Apoptosis under each condition was evaluated as described. If the apoptotic fraction was greater under nonadherent conditions than under adherent conditions, anoikis induction was inferred.

Statistical Analysis

Multiple independent experiments were done for each data set. Results are shown as the mean ± SD. Student's t test was used to identify significant differences between the control and experimental groups. The correlation between clinicopathological factors and HMGA1 expression was evaluated by the Fisher exact test with differences considered statistically significant at $p < 0.05$.

RESULTS

HMGA1 Expression

Human RCC tumor tissue (surgical specimens). HMGA1 expression in kidney tumor and normal kidney tissues from the same patient after radical nephrectomy was examined by immunoblot. Immunoblots of surgical samples from 48 cases of RCC revealed that HMGA1 was not expressed in normal kidney tissue in any case while HMGA1 was expressed in tumor tissue in 1 of 30 nonmetastatic (M0) (3%) and 6 of 18 metastatic (M1) (33%) cases ($p = 0.008$) as well as in 3 of 36 G1–2 (8%) and 4 of 9 G3 (44%) cases ($p = 0.022$, see table and fig. 1, *A*). These findings suggest the preferential expression of HMGA1 in high grade and metastatic RCC.

Human RCC cells. High HMGA1 expression was detected by immunoblot in Caki-1 cells derived from skin metastasis and in ACHN cells derived from pleural effusion. Low expression was detected in NC65 cells derived from moderately differentiated primary renal cancer whose host had skin metastasis. Scarcely detectable expression was noted in 786-O cells derived from primary renal cancer whose host had metastasis after nephrectomy, RCC-4 and A498 cells (fig. 1, *B*). Immunofluorescence revealed nuclear localization of HMGA1 in Caki-1, ACHN and NC65 cells (fig. 1, *C*). Significant HMGA1 expression was confirmed in ACHN and Caki-1 cells and, thus, these lines were subsequently used to examine HMGA1 function using RNA interference.

HMGA1 expression in RCC

	Total No.	No. Pos HMGA1 (%)	No. Neg HMGA1 (%)	p Value (Fisher exact test)
Kidney:				0.012
Normal	48	0	48 (100)	
Tumor	48	7 (15)	41 (85)	
Histological grade:				0.022
G1–2	36	3 (8)	33 (92)	
G3	9	4 (44)	5 (56)	
Metastasis clinical stage:				0.008
M0	30	1 (3)	29 (97)	
M1	18	6 (33)	12 (67)	

HMGA1 Knockdown

By siRNA. HMGA1 knockdown in Caki-1 and ACHN cells was achieved using HMGA1 specific siRNA. Immunoblot revealed that transient transfection with HMGA1 specific siRNA efficiently and significantly decreased HMGA1 expression in each cell line 2 days after transfection while scrambled control siRNA barely affected the HMGA1 level (fig. 2, *A*). These knockdown experiments were applied to the following experiments to evaluate HMGA1 function in the 2 cell lines.

Colony formation and cell proliferation inhibition. The effects of HMGA1 knockdown on cell growth and survival in Caki-1 and ACHN cells were examined using a colony formation assay. HMGA1 knockdown using HMGA1 specific siRNA in ACHN cells remarkably inhibited colony formation. However, transfecting control siRNA with a scrambled sequence scarcely affected the number of colonies (control vs HMGA1 siRNA mean 127.7 ± 5.4 vs 5.7 ± 2.5, $p < 0.01$, fig. 2, *B* and *C*). HMGA1 knockdown in Caki-1 cells also remarkably suppressed colony formation (control vs HMGA1 mean 86.0 ± 5.3 vs 7.3 ± 1.5, $p < 0.01$, fig. 2, *B* and *C*). Similarly HMGA1 knockdown in ACHN and Caki-1 cells remarkably suppressed cell proliferation (fig. 2, *D*).

Apoptosis induction. Since the results of our colony formation and cell proliferation assays suggested an inhibitory effect of HMGA1 knockdown on cell survival and growth, we examined how HMGA1 knockdown affected apoptosis induction. Transfection of HMGA1 specific siRNA induced significant apoptosis in ACHN and Caki-1 cells in a time dependent, siRNA sequence specific manner. Four days after transfection the mean ACHN sub-G1 fraction was 2.3% ± 0.4% vs 39.8% ± 0.7% and the mean Caki-1

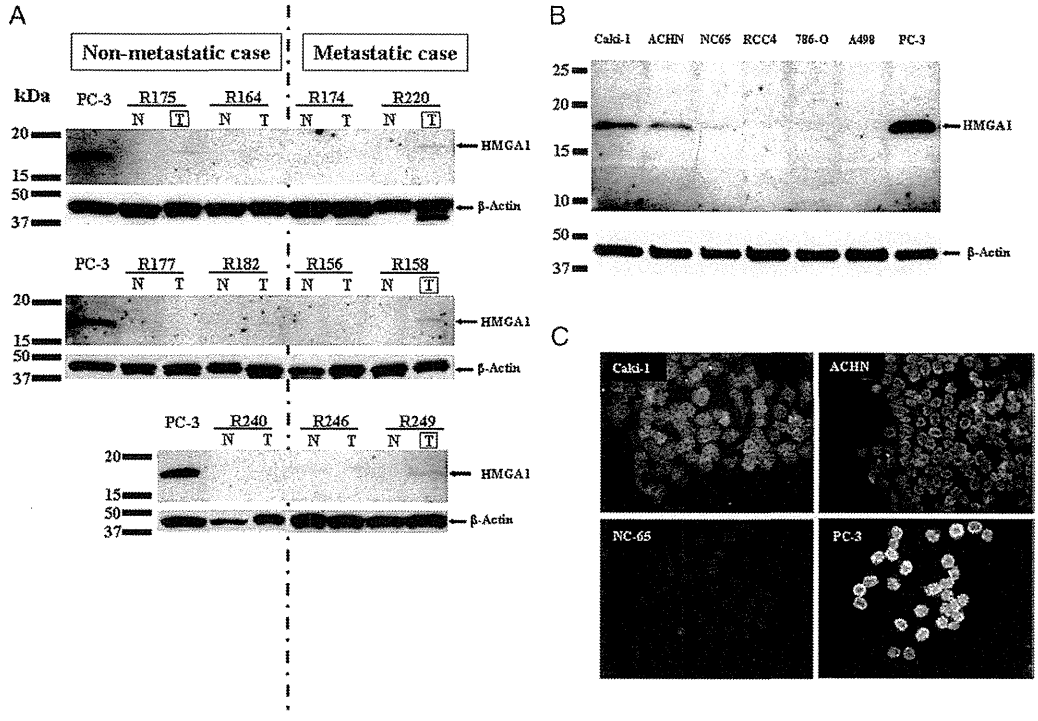

Figure 1. HMGA1 expression in RCC. PC-3 served as loading positive control. *A*, HMGA1 and β-actin expression in normal (*N*) and tumor kidney tissue from same patients was assessed by immunoblot. Boxed *T*, kidney tumor tissue expressing HMGA1. *T*, kidney tumor tissue with no HMGA1 expression. *B*, HMGA1 and β-actin expression in human RCC cell lines was assessed by immunoblot. *C*, immunofluorescence revealed HMGA1 nuclear localization in Caki-1, ACHN, NC-65 and PC-3 cells at different intensities.

sub-G1 fraction was 7.1% ± 1.0% vs 41.6% ± 1.7% for control siRNA vs HMGA1 specific siRNA, respectively (each $p < 0.01$, fig. 3, *A*). The blocking effect of the pancaspase inhibitor zVAD-fmk on apoptosis induction by HMGA1 knockdown was significant in ACHN but minimal in Caki-1 cells (fig. 3, *B*).

These findings suggest that HMGA1 has inhibitory effects on caspase independent and dependent apoptosis in RCC cells. The induction of apoptosis by transfection of HMGA1 specific siRNA in ACHN and Caki-1 cells was also confirmed by the emergence of annexin V positive cells (fig. 3, *C*).

Inhibition of ACHN cell in vitro invasion and migration. In vitro invasion assay after 24-hour incubation showed that the number of untreated ACHN cells invading the Matrigel coated membrane was high enough to be counted while that of untreated Caki-1 cells was not. Thus, the role of HMGA1 in cell invasion and migration was evaluated using ACHN cells.

In vitro invasion assay revealed that transfection of HMGA1 specific siRNA significantly decreased the number of ACHN cells invading the Matrigel coated membrane compared to the transfection of control siRNA (169.3 ± 10.1 vs 718.3 ± 163.5 cells, $p < 0.01$, fig. 4, *A*). Similarly our in vitro migration assay indicated that transfection of HMGA1 specific siRNA significantly decreased the number of ACHN cells migrating through the uncoated membrane compared to the transfection of control siRNA (299.0 ± 30.8 vs 590.0 ± 112.1 cells, $p < 0.05$, fig. 4, *B*).

Anoikis induction and phosphorylated Akt down-regulation in ACHN cells. Anoikis induction was first examined using untreated ACHN and Caki-1 cells. In each untreated cell line no significant increase was noted in apoptotic cells under nonadherent vs adherent culture conditions (fig. 5, *A*). Thus, the 2 cell lines were judged to be anoikis resistant. No significant anoikis was observed in ACHN cells transfected with control siRNA while significant anoikis was observed in ACHN cells transfected with HMGA1 specific siRNA (fig. 5, *B*). In contrast, no significant anoikis was induced in Caki-1 cells transfected with control or HMGA1 specific siRNA (fig. 5, *B*).

Since it was suggested in the literature that anoikis resistance is associated with Akt phosphorylation at Ser473, the phosphorylation of Akt in each cell line 4 days after siRNA transfection was examined by immunoblot analysis. In ACHN cells HMGA1 knockdown was associated with P-Akt down-regulation compared to transfection with control siRNA while total Akt expression was least affected by transfection of HMGA1 specific or control siRNA (fig. 5, *C*). Conversely HMGA1 knockdown in Caki-1

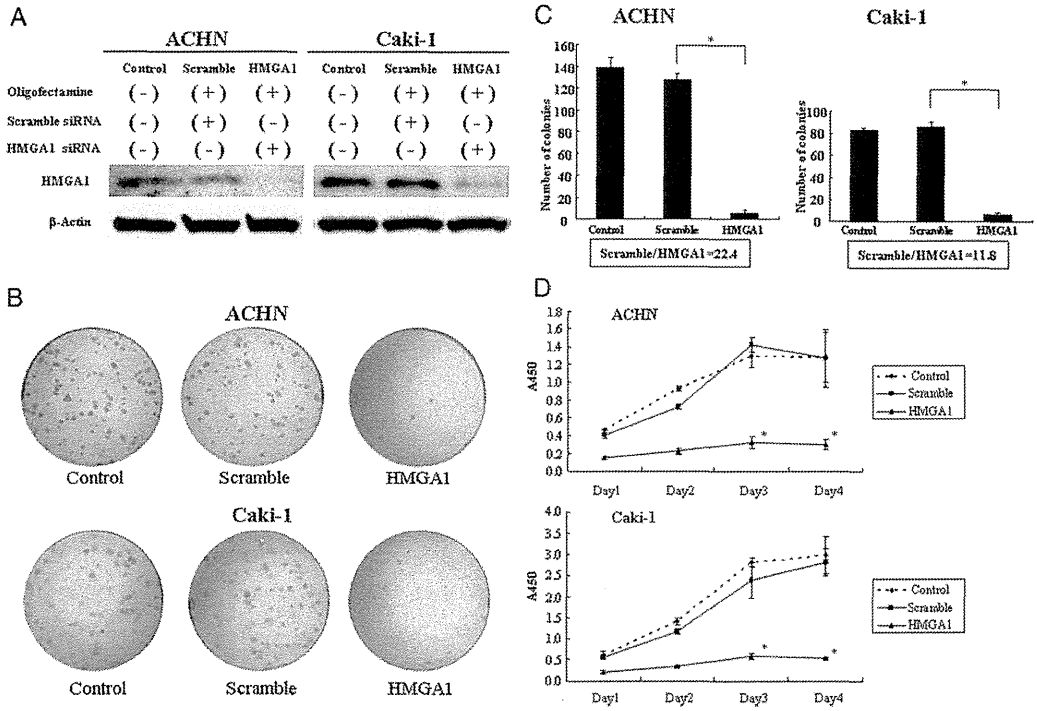

Figure 2. HMGA1 knockdown inhibited colony formation by RCC cells. *A*, expression of HMGA1 and β-actin as loading control in ACHN and Caki-1 cells was assessed by immunoblot. HMGA1 efficient decrease was confirmed in cells treated with HMGA1 specific siRNA (*HMGA1*) but not in cells treated with control siRNA (*Scramble*) vs untreated control cells. *B*, macroscopic appearance of ACHN and Caki-1 colonies treated with siRNA. Two days after siRNA transfection 150 cells were seeded per well. *C*, graphic presentation of the number of ACHN and Caki-1 colonies. Columns indicate mean of 3 preparations. Bars indicate SD. Asterisk indicates $p < 0.01$. *D*, ACHN and Caki-1 cell proliferation. Two days after transfection with siRNA on day 0 cells were seeded in 96-well plates for WST-8 assay on days 1 to 4. Points indicate mean of 6 preparations. Bars indicate SD. Asterisk indicates $p < 0.01$ vs cells treated with control siRNA.

cells did not lead to significant P-Akt down-regulation (fig. 5, *C*). These findings suggest that HMGA1 knockdown in cases associated with P-Akt down-regulation is involved in anoikis induction in a subset of RCC cells.

DISCUSSION

The introduction of molecular targeted drugs in clinical settings has conferred significant survival benefits for patients with mRCC but the antitumor effect of these drugs is relatively weak since they rarely achieve a complete response. Also, various side effects are commonly associated with molecular targeted drugs.[1] Identifying novel candidate target molecules with significant molecular functions is mandatory to develop new therapeutic modalities for mRCC. If the expression of these candidate molecules is observed exclusively in RCC cells but not in normal cells, the incidence of side effects should be minimal. In addition, if these candidate molecules have a significant role in cell growth or survival, therapy targeting and inhibiting these molecules should have significant antitumor effects. To this end we examined the expression and molecular function of HMGA1 in RCC cells.

HMGA1 expression is high in normal embryonic tissue but low or almost undetectable in adult tissue.[6] In contrast, HMGA1 is over expressed in cancer of various types, including cancer of the pancreas,[21] colon,[22] prostate,[13,14] ovary[23] and testis,[24] especially in association with high grade and metastasis.[2,5,21,25] HMGA1 is also a potent oncogene.[7,8,10,11] Furthermore, various important functions and roles in cancer have been reported for HMGA1. To our knowledge this is the first report to describe the expression and role of HMGA1 in RCC. We examined HMGA1 expression in RCC using surgical specimens and cell lines. We also estimated the molecular function of HMGA1 in RCC by HMGA1 knockdown using RNA interference.

HMGA1 was preferentially expressed in metastatic RCC tumor tissue and cell lines but not in normal tissue. Our functional analysis revealed that HMGA1 knockdown induced remarkable inhibition of colony formation and significant apoptosis in RCC cells. These findings make this molecule a candidate

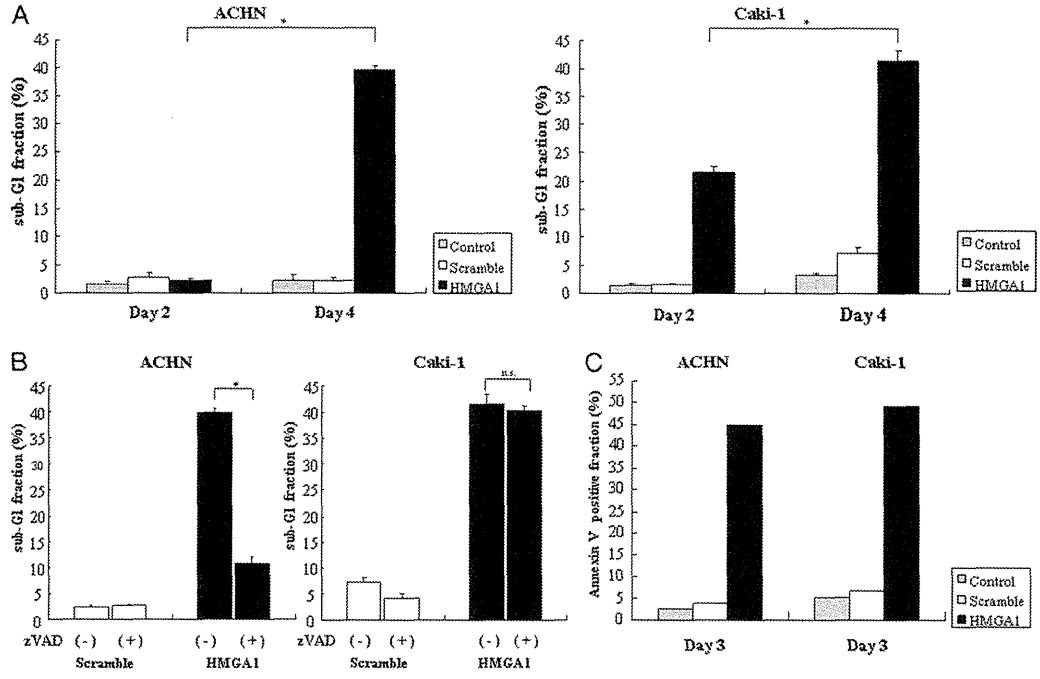

Figure 3. HMGA1 knockdown induced apoptosis in ACHN and Caki-1 RCC cells. siRNA treatment was done as described. *A* and *B*, apoptosis (sub-G1 fraction) was identified by flow cytometry. *A*, apoptosis time dependent induction. *B*, effect of pancaspase inhibitor zVAD-fmk on apoptosis. *C*, representative flow cytometry data on apoptosis. Apoptosis was evaluated by percent of annexin V positive fraction 3 days after siRNA transfection. *Scramble*, cells treated with control siRNA. Columns indicate mean of 3 preparations. Bars indicate SD. *n.s.*, not statistically significant ($p > 0.05$). Asterisk indicates $p < 0.01$.

for molecular targeted therapy for mRCC and suggest a significant antitumor effect with minimal side effects.

Our study also suggests that HMGA1 has a role in the metastatic cascade, including the acquisition of invasion potential and anoikis resistance. After cancer cells detach from a primary site upon acquiring invasion potential they must survive anoikis to develop metastatic lesions. Resistance to anoikis or detachment induced apoptosis was suggested as a phenotypic hallmark of metastatic cancer cells.[26] The PI3 kinase/Akt pathway activation is reportedly involved in resistance to anoikis.[26]

Notably Liau et al reported that HMGA1 in pancreatic cancer cells is involved in anoikis resistance and associated with Akt activation.[20] Our study suggests that HMGA1 knockdown in cases associated with P-Akt down-regulation is involved in anoikis

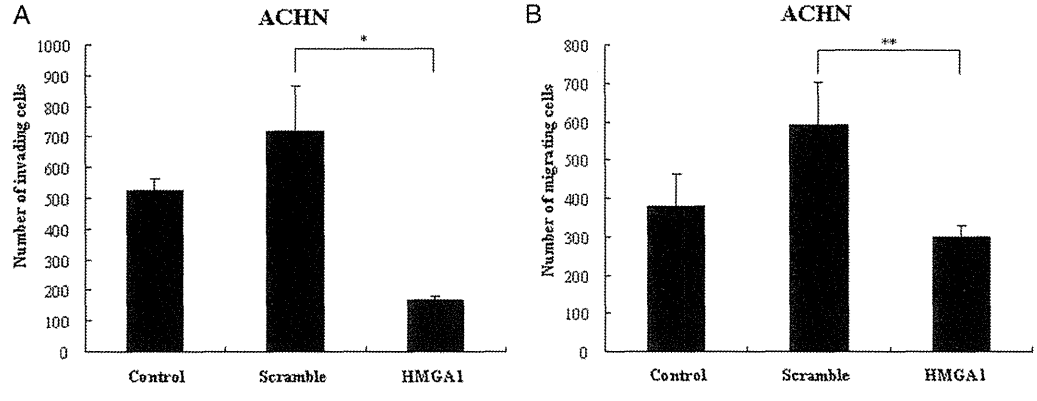

Figure 4. HMGA1 knockdown inhibited ACHN cell invasion and migration in vitro. siRNA treatment was done as described. *Scramble*, cells treated with control siRNA. Columns indicate mean of 3 preparations. Bars indicate SD. *A*, asterisk indicates $p < 0.01$. *B*, asterisks indicate $p < 0.05$.

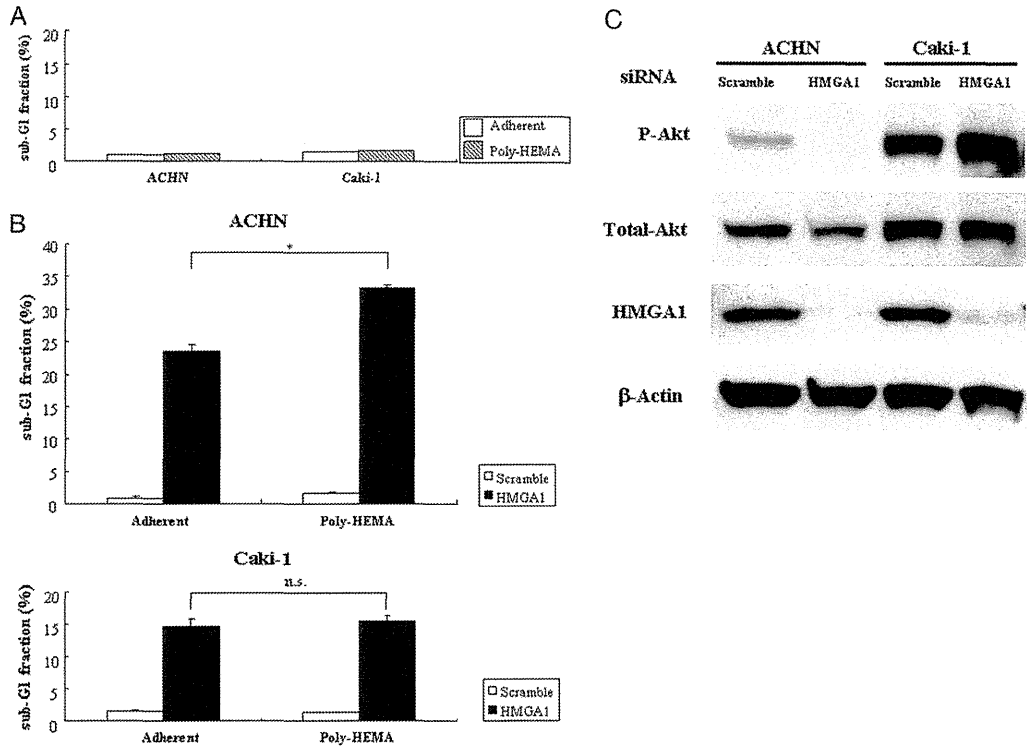

Figure 5. HMGA1 knockdown affected RCC cell anoikis. siRNA treatment was done as described. *A*, ACHN and Caki-1 were resistant to anoikis. No increase in apoptosis under nonadherent conditions with poly-HEMA was noted vs adherent conditions in each cell line. *B*, HMGA1 knockdown induced significant anoikis in ACHN but not in Caki-1 cells. *Scramble*, cells treated with control siRNA. Columns indicate mean of 3 preparations. Bars indicate SD. *n.s.*, not statistically significant ($p > 0.05$). Asterisk indicates $p < 0.01$. *C*, immunoblot produced using antibodies against P-Akt, total Akt, HMGA1 and β-actin showed that HMGA1 knockdown led to down-regulation of P-Akt associated with anoikis induction in ACHN but not Caki-1 cells.

induction in RCC cells. This indicates that therapy targeting HMGA1 could inhibit the formation of metastatic lesions that develop from existing metastatic lesions, which would significantly affect the survival of patients with mRCC.

Several drugs that affect HMGA1 DNA binding activity have been examined to estimate their efficacy and toxicity in animal models and clinical trials, including distamycin, FR900482, FK317, netropsin and NOX-A50.[27,28] Alternatively other groups have targeted important molecules downstream of HMGA1, including COX-2, STAT3 and MMP-2.[29] HMGA1 has multiple important biological roles in cancer cells, including oncogenic activity in vitro[7,8] and in vivo,[10,11] cell growth,[8,15] metastatic potential,[5,7,14,16] chromosomal rearrangement,[17] and p53[3] and Rb[4] inhibition, in addition to the regulation of gene expression.[2] Thus, antisense therapy for HMGA1 that suppresses the expression of only 1 gene would produce multiple effects simultaneously, which might contribute greatly to mRCC control. Chi et al developed an antisense construct for clusterin and applied it clinically to treat castration resistant prostate cancer.[30] Further in vivo studies and the development of an antisense construct are warranted to confirm whether HMGA1 is a good candidate molecule for targeted therapy of mRCC.

CONCLUSIONS

HMGA1 was preferentially expressed in mRCC but not expressed in normal kidney tissue. Functional analysis revealed that HMGA1 knockdown markedly inhibited colony formation, significantly induced apoptosis, inhibited invasion potential and induced anoikis. These findings suggest that HMGA1 is a potential target molecule for novel molecular targeted therapy of mRCC.

ACKNOWLEDGMENTS

Y. Morioka, C. Tsukisato, K. Koishihara and M. Nishida provided technical assistance.

REFERENCES

1. Bastien L, Culine S, Paule B et al: Targeted therapies in metastatic renal cancer in 2009. BJU Int 2009; **103:** 1334.
2. Fusco A and Fedele M: Roles of HMGA proteins in cancer. Nat Rev Cancer 2007; **7:** 899.
3. Frasca F, Rustighi A, Malaguarnera R et al: HMGA1 inhibits the function of p53 family members in thyroid cancer cells. Cancer Res 2006; **66:** 2980.
4. Ueda Y, Watanabe S, Tei S et al: High mobility group protein HMGA1 inhibits retinoblastoma protein-mediated cellular G0 arrest. Cancer Sci 2007; **98:** 1893.
5. Evans A, Lennard TW and Davies BR: High-mobility group protein 1(Y): metastasis-associated or metastasis-inducing? J Surg Oncol 2004; **88:** 86.
6. Chiappetta G, Avantaggiato V, Visconti R et al: High level expression of the HMGI (Y) gene during embryonic development. Oncogene 1996; **13:** 2439.
7. Wood LJ, Maher JF, Bunton TE et al: The oncogenic properties of the HMG-I gene family. Cancer Res 2000; **60:** 4256.
8. Wood LJ, Mukherjee M, Dolde CE et al: HMG-I/Y, a new c-Myc target gene and potential oncogene. Mol Cell Biol 2000; **20:** 5490.
9. Tesfaye A, Di Cello F, Hillion J et al: The high-mobility group A1 gene up-regulates cyclooxygenase 2 expression in uterine tumorigenesis. Cancer Res 2007; **67:** 3998.
10. Fedele M, Pentimalli F, Baldassarre G et al: Transgenic mice overexpressing the wild-type form of the HMGA1 gene develop mixed growth hormone/prolactin cell pituitary adenomas and natural killer cell lymphomas. Oncogene 2005; **24:** 3427.
11. Xu Y, Sumter TF, Bhattacharya R et al: The HMG-I oncogene causes highly penetrant, aggressive lymphoid malignancy in transgenic mice and is overexpressed in human leukemia. Cancer Res 2004; **64:** 3371.
12. Liau SS, Jazag A and Whang EE: HMGA1 is a determinant of cellular invasiveness and in vivo metastatic potential in pancreatic adenocarcinoma. Cancer Res 2006; **66:** 11613.
13. Tamimi Y, van der Poel HG, Denyn MM et al: Increased expression of high mobility group protein I(Y) in high grade prostatic cancer determined by in situ hybridization. Cancer Res 1993; **53:** 5512.
14. Tamimi Y, van der Poel HG, Karthaus HF et al: A retrospective study of high mobility group protein I(Y) as progression marker for prostate cancer determined by in situ hybridization. Br J Cancer 1996; **74:** 573.
15. Takaha N, Resar LM, Vindivich D et al: High mobility group protein HMGI(Y) enhances tumor cell growth, invasion, and matrix metalloproteinase-2 expression in prostate cancer cells. Prostate 2004; **60:** 160.
16. Leman ES, Madigan MC, Brunagel G et al: Nuclear matrix localization of high mobility group protein I(Y) in a transgenic mouse model for prostate cancer. J Cell Biochem 2003; **88:** 599.
17. Takaha N, Hawkins AL, Griffin CA et al: High mobility group protein I(Y): a candidate architectural protein for chromosomal rearrangements in prostate cancer cells. Cancer Res 2002; **62:** 647.
18. Uchiyama H, Sowa Y, Wakada M et al: Cyclin-dependent kinase inhibitor SU9516 enhances sensitivity to methotrexate in human T-cell leukemia Jurkat cells. Cancer Sci 2010; **101:** 728.
19. Kolb S, Fritsch R, Saur D et al: HMGA1 controls transcription of insulin receptor to regulate cyclin D1 translation in pancreatic cancer cells. Cancer Res 2007; **67:** 4679.
20. Liau SS, Jazag A, Ito K et al: Overexpression of HMGA1 promotes anoikis resistance and constitutive Akt activation in pancreatic adenocarcinoma cells. Br J Cancer 2007; **96:** 993.
21. Hristov AC, Cope L, Di Cello F et al: HMGA1 correlates with advanced tumor grade and decreased survival in pancreatic ductal adenocarcinoma. Mod Pathol 2010; **23:** 98.
22. Abe N, Watanabe T, Sugiyama M et al: Determination of high mobility group I(Y) expression level in colorectal neoplasias: a potential diagnostic marker. Cancer Res 1999; **59:** 1169.
23. Masciullo V, Baldassarre G, Pentimalli F et al: HMGA1 protein over-expression is a frequent feature of epithelial ovarian carcinomas. Carcinogenesis 2003; **24:** 1191.
24. Franco R, Esposito F, Fedele M et al: Detection of high-mobility group proteins A1 and A2 represents a valid diagnostic marker in post-pubertal testicular germ cell tumours. J Pathol 2008; **214:** 58.
25. Ben-Porath I, Thomson MW, Carey VJ et al: An embryonic stem cell-like gene expression signature in poorly differentiated aggressive human tumors. Nat Genet 2008; **40:** 499.
26. Sakamoto S, McCann RO, Dhir R et al: Talin1 promotes tumor invasion and metastasis via focal adhesion signaling and anoikis resistance. Cancer Res 2010; **70:** 1885.
27. Beckerbauer L, Tepe JJ, Eastman RA et al: Differential effects of FR900482 and FK317 on apoptosis, IL-2 gene expression, and induction of vascular leak syndrome. Chem Biol 2002; **9:** 427.
28. Maasch C, Vater A, Buchner K et al: Polyethyelenimine-polyplexes of Spiegelmer NOX-A50 directed against intracellular high mobility group protein A1 (HMGA1) reduce tumor growth in vivo. J Biol Chem 2010; **285:** 40012.
29. Resar LM: The high mobility group A1 gene: transforming inflammatory signals into cancer? Cancer Res 2010; **70:** 436.
30. Chi KN, Hotte SJ, Yu EY et al: Randomized phase II study of docetaxel and prednisone with or without OGX-011 in patients with metastatic castration-resistant prostate cancer. J Clin Oncol 2010; **28:** 4247.

Significant induction of apoptosis in renal cell carcinoma cells transfected with cationic multilamellar liposomes containing the human interferon-β gene through activation of the intracellular type 1 interferon signal pathway

NATSUKI TAKAHA[1,2], HIROYUKI NAKANISHI[1], YASUNORI KIMURA[1], FUMIYA HONGO[1], KAZUMI KAMOI[1], AKIHIRO KAWAUCHI[1], MASAAKI MIZUNO[3], JUN YOSHIDA[4], TOSHIHIKO WAKABAYASHI[5] and TSUNEHARU MIKI[1,2]

Departments of [1]Urology and [2]Translational Cancer Drug Development, Kyoto Prefectural University of Medicine, Kawaramachi-Hirokoji, Kyoto 602-8566; [3]Center for Advanced Medicine and Clinical Research, Nagoya University Hospital, 65 Tsurumai-cho, Showa-ku, Nagoya 466-8560; [4]Chubu Rosai Hospital, 1-10-6 Komei, Minato-ku, Nagoya 455-8530; [5]Neurosurgery, Nagoya University, Graduate School of Medicine, 65 Tsurumai-cho, Showa-ku, Nagoya 466-8550, Japan

Received October 30, 2011; Accepted December 22, 2011

DOI: 10.3892/ijo.2012.1377

Abstract. We previously reported that cationic multilamellar liposome containing the human interferon-β *(huIFN-β)* gene (IAB-1) demonstrated significant cytotoxic effect in the NC65 human renal cell carcinoma (RCC) cell line. In this study, we investigated the molecular mechanisms of IAB-1-induced apoptosis and cytotoxicity in RCC cells. Remarkable *in vitro* cytotoxic and apoptosis-inducing effects of IAB-1 against NC65 cells were observed by a colorimetric method and TUNEL staining, respectively. In contrast, treatment of NC65 cells with exogenously added huIFN-β protein induced low-level cytotoxicity without apoptosis. Neutralizing antibodies against huIFN-β significantly suppressed the cytotoxic effect of huIFN-β protein, but they were unable to block the effect of IAB-1. Cytotoxicity assays using transwell plates revealed that NC65 cells treated with IAB-1 did not secrete cytotoxic soluble factors other than IFN-β. Substantial enhancement of interferon-stimulated response element (ISRE) activity of NC65 cells by IAB-1 was demonstrated by promoter reporter assays. In addition, immunofluorescence using confocal microscopy revealed the intracellular expression of IFN-β and its receptor induced by IAB-1. The induction of c-Myc by IAB-1 was suggested by a cDNA macroarray and was confirmed by western blot analysis. These findings indicate that IAB-1 induces significant cytotoxicity and apoptosis in NC65 cells, possibly through enhanced ISRE activity, that is associated with increased intracellular localization of huIFN-β and IFN-receptor. Our data support the potential clinical application of IAB-1 gene therapy for RCC resistant to IFN.

Correspondence to: Dr Natsuki Takaha, Departments of Urology and Translational Cancer Drug Development, Kyoto Prefectural University of Medicine, Kawaramachi-Hirokoji, Kyoto 602-8566, Japan
E-mail: ntakaha@koto.kpu-m.ac.jp

Abbreviations: hu, human; IFN, interferon; PBS, phosphate-buffered saline; RCC, renal cell carcinoma; OD, optical density; TUNEL, terminal deoxynucleotidyl transferase-mediated dUTP nick end-labeling; STAT, signal transducer and activator of transcription; ISGF, interferon-stimulated gene factor; ISRE, interferon-stimulated response element; SD, standard deviation

Key words: apoptosis, gene therapy, IAB-1, IFN-β, renal cell carcinoma

Introduction

There are few effective therapeutic modalities for metastatic renal cell carcinoma (RCC). Among these treatment strategies, interferons (IFNs) have generally been included. Many combination treatments with other biological agents and chemotherapeutic agents have been developed to enhance the effectiveness of IFNs. However, response rates to these therapies have been reported to be ~15-20% (1-4), which is not satisfactory. Although molecular-targeted therapy has recently been introduced to treat metastatic renal cell carcinoma (mRCC) patients and has been shown to improve clinical outcome, a complete response has rarely been observed, and the therapy has various adverse effects (5-8). Therefore, the prognosis of mRCC remains poor, emphasizing the need to develop novel therapeutic modalities. One such promising treatment involves gene therapy.

We previously reported that cationic multilamellar liposomes containing the *IFN-β* gene (IAB-1) show significant antitumor activity against RCC both *in vitro* and *in vivo* (9).

Significant cytotoxic effects as well as apoptosis are induced by IAB-1, but not by the huIFN-β protein. Therefore, we speculated that one mechanism of enhanced cytotoxicity by IAB-1 may be via the induction of apoptosis. We even observed cytotoxicity and apoptosis against the relatively IFN-β protein-resistant NC65 cell line, which suggests that this method may be suitable for clinical application to treat IFN-resistant RCC. Elucidation of the molecular mechanisms of IAB-1-induced apoptosis and cytotoxicity in RCC cells would be useful for developing and optimizing effective gene therapies for RCC. In this study, we examined the molecular mechanisms responsible for the significant apoptosis and cytotoxicity of RCC cells induced by IAB-1.

Materials and methods

Cells. The human RCC cell line NC65 (10) was maintained in RPMI-1640 medium (Life Technologies Inc., Gaithersburg, MD, USA) supplemented with 100 U/ml penicillin, 100 μg/ml streptomycin (Life Technologies Inc.), and 10% heat-inactivated fetal bovine serum (Life Technologies Inc., Bio-cult, Glasgow, Scotland, UK), hereafter referred to as complete medium.

Reagents. IAB-1 is a plasmid DNA/lipid complex composed of a plasmid (pSV2IFNβ) that contains the SV40 early promoter and the *huIFN-β* gene coding sequence (11), and positively charged liposomes [N-(α-trimethylammonioacetyl)-didodecyl-D-glutamine chloride, dilauroyl phosphatidylcholine, and dioleoyl phosphatidylethanolamine in a molar ratio of 1:2:2], as described previously (11-13). The final concentration of IAB-1 was 50 nmol of lipid/μl with 1.0 μg plasmid DNA/μl. The empty liposome was composed of liposome alone (50 nmol of lipid/μl) without plasmid DNA (9). The IAB-1 and empty liposomes were dissolved in phosphate-buffered saline (PBS) and diluted to the indicated concentrations. Recombinant huIFN-β protein (IFN-β Mochida, 2.0×10^5 IU/mg) was provided from Mochida Pharmaceutical Inc., Tokyo, Japan (9). Neutralizing anti-huIFN-β monoclonal antibody (clone 76703.111) was purchased from R&D Systems Inc. (Minneapolis, MN, USA).

IFN-β gene transfer. Aliquots of 5.0×10^4 cultured cells were placed in each well of 6-well plates with 2 ml medium and were incubated for 24 h at 37°C in a humidified atmosphere of 5% CO_2 (standard conditions). IAB-1 solution or empty liposome solution was then added, and incubation was continued for up to 3 days (9,14).

Cytotoxicity assay. Cytotoxicity was evaluated by a colorimetric method using 2-(2-methoxy-4-nitrophenyl)-3-(4-nitrophenyl)-5-(2, 4-disulfophenyl)-2H-tetrazolium monosodium salt (WST-8; Nacalai Tesque, Kyoto, Japan) (15). Briefly, triplicate aliquots of cells were treated with IAB-1. After incubation under standard conditions, the culture supernatant was replaced with 1 ml fresh complete medium containing 0.5 μmol tetrazolium salt. After incubation for an additional 1 h, culture supernatants were harvested, and the optical density (OD) at 450 nm was measured. Cytotoxicity was calculated as follows: cytotoxicity (%) = [1 - (absorbance of experimental wells/average absorbance of control wells)] x100 (9).

Terminal deoxynucleotidyl transferase-mediated dUTP nick end-labeling (TUNEL) assay for detection of apoptotic cells. Apoptosis was examined by the TUNEL method, as previously reported (16). NC65 cells were incubated with 0.1 μl/ml IAB-1 (5.0 nmol lipid with 0.1 μg plasmid DNA/ml) or 10000 IU/ml recombinant huIFN-β protein for 24 h under standard conditions. After incubation, apoptotic cells were detected using an *in situ* Apoptosis Detection kit (Takara, Otsu, Japan), according to the manufacturer's protocol. Labeled cells were observed with a fluorescence microscope (16).

Western blot analysis. Sample proteins (20 μg) were separated on 10% polyacrylamide gels in Tris-glycine buffer and transferred onto nitrocellulose membranes. The nitrocellulose membranes were blocked for 30 min with blocking buffer (5% skim milk in 0.1% Tween-PBS) and probed with anti-c-Myc monoclonal antibody (clone 9E10; Santa Cruz Biotechnology, Santa Cruz, CA, USA), anti-signal transducer and activator of transcription 1 (STAT1) monoclonal antibody (clone 42; BD Biosciences, San Jose, CA, USA), anti-STAT2 monoclonal antibody (clone 22; BD Biosciences), or anti-interferon-stimulated gene factor 3γ (ISGF3γ, p48) monoclonal antibody (clone 6; BD Biosciences) for 1 h. The membrane was washed and then incubated with alkaline phosphatase-conjugated goat anti-mouse IgG (Sigma, St. Louis, MO, USA). The signal was detected with the BCIP-NBT kit (Nacalai Tesque). The relative expression of c-Myc, STAT1, STAT2, and ISGF3 was determined with Gel Doc 2000 (Bio-Rad Laboratories, Osaka, Japan).

The measurement of interferon-stimulated response element (ISRE) activity. The activity of ISRE in NC65 cells treated with IAB-1 or recombinant huIFN-β protein was measured using Pathway Profiling Luciferase System 5 (Clontech Laboratories Inc., Mountain View, CA, USA), according to the manufacturer's protocol. pISRE-Luc is a signal transduction *cis*-reporter vector. It was designed to monitor the activation of IFN-triggered signal transduction pathways. pISRE-Luc contains five copies of the ISRE-binding sequence, located upstream of the TATA-like promoter (P_{TAL}) region of the herpes simplex virus thymidine kinase promoter. Located downstream from P_{TAL} is the firefly *luciferase* reporter gene. After activated transcription factors bind to the *cis*-acting enhancer element, ISRE, transcription is induced and the *luciferase* reporter gene is activated. The activity of luciferase is proportional to the level of induction of cellular gene transcription by type 1 IFN. pTA-Luc, the negative control plasmid vector, was used as a control.

NC65 cells were plated the day before transfection of the Pathway Profiling Luciferase vectors. Then, 1 μg pISRE-Luc or pTA-Luc was transfected with 9 μg SuperFect transfection reagent (Qiagen, Hilden, Germany), according to the manufacturer's protocol. One day after the transfection, IAB-1 or recombinant huIFN-β protein was added to the wells, as described above in '*IFN-β* gene transfer', and the cells were incubated for 24 h. Luciferase activity was measured using a Luciferase assay kit (Promega, Madison, WI, USA), according to the manufacturer's protocol. Photoemission was measured for 10 sec using a luminometer.

Fluorescent confocal imaging of IFN-β protein and type 1 IFN-receptor. NC65 cells were treated with IAB-1 or huIFN-β

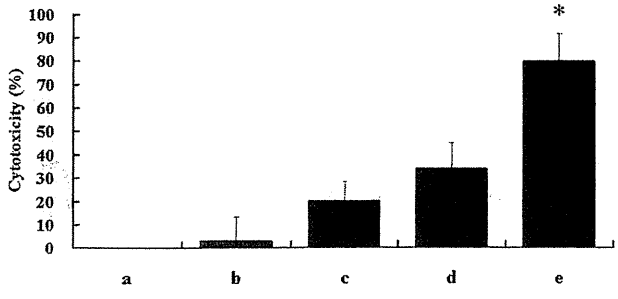

Figure 1. Cytotoxicity of IAB-1 against NC65 *in vitro*. NC65 cells ($1.25x10^4$) were placed in each well of a 24-well plate with 0.5 ml medium and incubated for 24 h. PBS (control), recombinant huIFN-β protein, empty liposome, or IAB-1 was added to the medium, and the cells were further incubated for 3 days. Cytotoxicity was evaluated by a colorimetric method using tetrazolium salt as described in Materials and methods. a, control (PBS); b, 0.1 μl/ml of empty liposome (5.0 nmol lipid/ml); c, 1000 IU/ml recombinant huIFN-β; d, 0.01 μl/ml of IAB-1 (0.5 nmol lipid with 0.01 μg plasmid DNA/ml); e, 0.1 μl/ml of IAB-1 (5.0 nmol lipid with 0.1 μg plasmid DNA/ml). Results were derived from three independent experiments and are expressed as mean ± SD. *p<0.05, compared to other treatment groups.

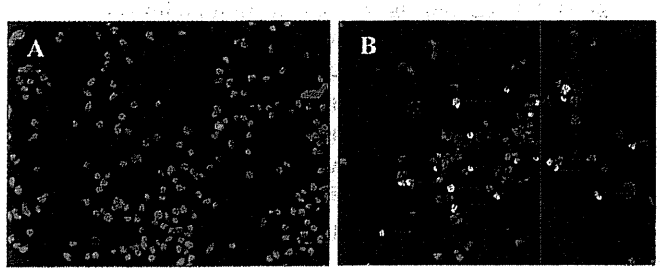

Figure 2. TUNEL assay for detection of apoptosis. NC65 cells were treated with (A) 10000 IU/ml recombinant huIFN-β protein or (B) 0.1 μl/ml of IAB-1 (5.0 nmol lipid with 0.1 μg plasmid DNA/ml). Apoptotic cells (yellow) were determined by TUNEL staining 24 h after treatment and visualized by fluorescence microscopy at x200 magnification. Red arrows indicate representative apoptotic cells.

protein in single-well chamber slides. After 24 h of incubation, the cells were fixed in 4% paraformaldehyde, permeabilized with 0.2% Triton X-100 in PBS, and then incubated with 1:25 mouse monoclonal anti-huIFN-β antibody (clone 76703.111; R&D Systems Inc.) and 1:10 rabbit polyclonal anti-IFNα/βRβ antibody (the beta chain of type 1 IFN-receptor, C-18; Santa Cruz Biotechnology) for 1 h at room temperature. After washing with PBS twice, the slides were incubated with AlexaFlour 488 goat anti-mouse IgG antibody (Invitrogen Corp., Carlsbad, CA, USA) and AlexaFlour 568 goat anti-rabbit IgG antibody (Invitrogen Corp.) at a dilution of 1:200 for 45 min. Slides were washed in PBS and coverslipped. Cells were viewed at x600 magnification. Images were collected with an Olympus Fluoview laser scanning confocal microscope (Olympus).

cDNA macroarray. Gene expression profiles using mRNA from NC65 cells treated with medium, 10000 IU/ml recombinant huIFN-β protein, 0.1 μl/ml empty liposome solution, or 0.1 μl/ml IAB-1 were compared by Atlas Human Cancer 1.2 Array (Clontech Laboratories Inc.). This array includes 1185 human genes. Cells were harvested 48 h after each treatment.

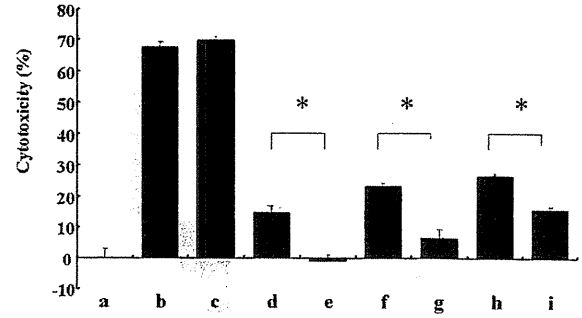

Figure 3. Neutralization effect of anti-IFNβ antibody on cytotoxicity of IAB-1 against NC65 *in vitro*. NC65 cells ($2.5x10^4$) were placed in each well of a 12-well plate with 1.0 ml medium and incubated for 24 h. PBS (control), recombinant huIFN-β protein, or IAB-1 was added to the medium with or without 20 μg/ml anti-huIFN-β monoclonal antibody (Ab). After 2 days of incubation, cytotoxicity was evaluated by a colorimetric method using tetrazolium salt as described in Materials and methods. a, control (PBS); b, 0.1 μl/ml of IAB-1 (5.0 nmol lipid with 0.1 μg plasmid DNA/ml); c, 0.1 μl/ml of IAB-1 + Ab; d, 100 IU/ml IFN-β; e, 100 IU/ml IFN-β + Ab; f, 1000 IU/ml IFN-β; g, 1000 IU/ml IFN-β + Ab; h, 10000 IU/ml IFN-β; i, 10000 IU/ml IFN-β + Ab. Results are expressed as mean ± SD (n=4 per treatment group). *p<0.05, comparing cells with antibody versus those without.

Statistical analysis. Multiple independent experiments were performed for each data set, and the results are presented as the mean ± standard deviation (SD). For statistical analysis, unpaired t-tests were used. Differences were considered statistically significant at $p<0.05$.

Results

Transfection of IAB-1 induces significant cytotoxicity and apoptosis in the human RCC line NC65. The cytotoxicity against NC65 cells induced after 3 days of incubation with 0.1 μl/ml IAB-1 was substantially higher than that after exogenously adding 1000 IU/ml recombinant huIFN-β protein (Fig. 1), consistent with our previous report (9). However, we previously found that NC65 cells treated with IAB-1 secreted IFN-β protein, and the concentration of IFN-β protein in the culture medium of NC65 cells treated with 0.1 μl/ml IAB-1 was consistently lower than that of cells treated with 1000 IU/ml recombinant huIFN-β protein (9). In this study, TUNEL staining demonstrated that transfection of 0.1 μl/ml IAB-1 significantly induced apoptosis, while treatment of NC65 cells with 10000 IU/ml recombinant huIFN-β protein did not (Fig. 2), which is also consistent with our previous study (9). These findings suggest that the ability of IAB-1 to induce cytotoxicity and apoptosis is not simply the result of IFN-β protein secretion.

Secreted huIFN-β protein is not the sole cause of cytotoxicity in IAB-1-transfected NC65 cells. Utilizing neutralization antibodies against huIFN-β, we evaluated the contribution of secreted huIFN-β protein to the cytotoxic and apoptotic effects of IAB-1. Neutralizing antibodies to huIFN-β protein significantly suppressed the cytotoxic effect of exogenously supplied huIFN-β protein, but did not block the lysis of IAB-1-transfected NC65 cells (Fig. 3). These results suggest that secreted huIFN-β protein was not the sole factor that induced cytotoxicity or apoptosis of IAB-1-transfected NC65 cells.

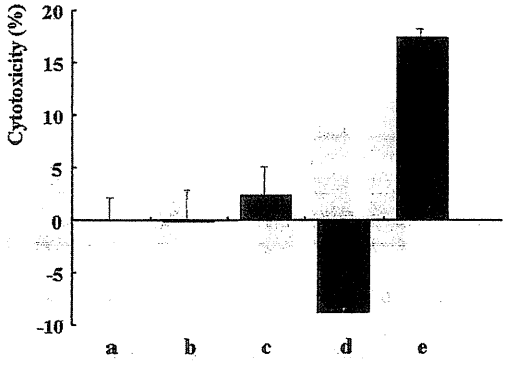

Figure 4. Effects of soluble factors secreted by IAB-1-transfected NC65 cells on untransfected NC65 cells using transwell plates. NC65 cells ($5.0x10^4$) were seeded in each compartment of a transwell plate (6-well plate). Two days after the addition of PBS (control), empty liposomes, IAB-1, or huIFN-β protein to the upper wells, the growth of NC65 cells in the lower wells was determined and cytotoxicity was evaluated by a colorimetric method using tetrazolium salt as described in Materials and methods. a, control (PBS); b, 0.1 μl/ml of empty liposome (5.0 nmol lipid/ml); c, 0.01 μl/ml of IAB-1 (0.5 nmol lipid with 0.01 μg plasmid DNA/ml); d, 0.1 μl/ml of IAB-1 (5.0 nmol lipid with 0.1 μg plasmid DNA/ml); e, 1000 IU/ml recombinant huIFN-β.

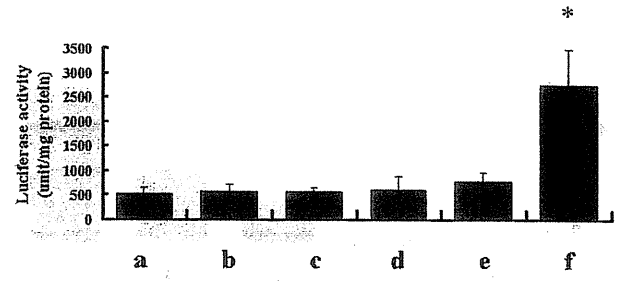

Figure 5. Activation of ISRE by IAB-1. NC65 cells were plated 1 day prior to transfection with control or ISRE promoter luciferase vectors. One day post-transfection, IAB-1 or recombinant huIFN-β protein was added to the wells, and the cells were incubated for an additional 24 h before measuring luciferase activity. a, control (PBS); b, 100 IU/ml recombinant huIFN-β; c, 1000 IU/ml recombinant huIFN-β; d, 10000 IU/ml recombinant huIFN-β; e, 0.01 μl/ml of IAB-1 (0.5 nmol lipid with 0.01 μg plasmid DNA/ml); f, 0.1 μl/ml of IAB-1 (5.0 nmol lipid with 0.1 μg plasmid DNA/ml). Results are expressed as mean ± SD (a-d, n=3; e and f, n=6). *$p<0.05$, compared to other treatment groups.

Lack of evidence for other cytotoxic or pro-apoptotic soluble factors secreted by IAB-1-transfected NC65 cells. To examine if IAB-1-transfected NC65 cells secreted other molecules that contributed to autocrine-mediated induction of cell lysis or apoptosis, we employed a transwell system, which is composed of two compartments (upper and lower) separated by a 1-mm space containing a polycarbonate membrane with 8.0 μm pores. NC65 cells were seeded into both compartments at $5.0x10^4$ cells/well (6-well plate), and IAB-1 or huIFN-β protein was added to the upper wells. Two days after the addition of IAB-1 or huIFN-β protein, the growth of NC65 cells in the lower well was determined and cytotoxicity was evaluated. Using this system, molecules secreted from the IAB-1-transfected NC65 cells in the upper wells transfer through the porous membrane and affect NC65 cells in the lower wells. IAB-1-transfected NC65 cells in the upper wells resulted in lower cytotoxicity of NC65 cells in the lower wells compared to huIFN-β protein-treated cells (Fig. 4). This suggests that IAB-1 does not induce the secretion of soluble factors, other than IFN-β, that significantly impact cell growth or cytotoxicity.

No difference in STAT1, STAT2, or p48 expression between IAB-1-transfected NC65 cells and huIFN-β protein-treated NC65 cells. We next examined the expression of ISGF3, which transduces signals triggered by IFN/IFN-receptor interactions through the cytoplasm and into the nucleus, activating the ISRE. ISGF3 consists of STAT1, STAT2, and p48, and their expression in NC65 cells treated with PBS or empty liposome solution was detected at very low levels by western blot analysis. In contrast, the expression of STAT1, STAT2, and p48 in NC65 cells was upregulated by the addition of 1000 IU/ml huIFN-β protein or 0.1 μl/ml IAB-1, but their levels of expression did not significantly differ between the two treatment groups (data not shown).

The activity of ISRE is enhanced by IAB-1. ISRE is a signal transduction *cis*-acting response element that is activated through IFN-triggered signal transduction pathways to induce the transcription of type 1 IFN-responsive genes. The addition of 0.1 μl/ml IAB-1 induced significant activation of ISRE, whereas 0.01 μl/ml IAB-1 or various concentrations of huIFN-β protein did not activate ISRE (Fig. 5). Luciferase activity was not demonstrated in control transfected with pTA-Luc (data not shown). These results suggest that the IFN-triggered signal transduction pathway is significantly activated in IAB-1-transfected NC65 cells.

IAB-1-induced intracellular expression of IFN-β and IFN-receptor. To further investigate the molecular mechanisms of IAB-1-induced apoptosis and cytotoxicity, compared to those of exogenously added huIFN-β protein, we examined the expression of huIFN-β protein and type 1 IFN-receptor by immunofluorescence. Confocal microscopy enabled us to assess the subcellular expression patterns of huIFN-β protein and type 1 IFN-receptor. In PBS-treated NC65 cells, type 1 IFN-receptor was expressed only on the cell membrane (Fig. 6A). When NC65 cells were treated with huIFN-β protein, huIFN-β protein and type 1 IFN-receptor were also detected on the cell membrane (Fig. 6A). In contrast, in IAB-1-treated NC65 cells, huIFN-β protein and type 1 IFN-receptor were observed predominantly in the cytoplasm and were co-localized (Fig. 6A and B).

c-Myc expression is enhanced by IAB-1. To better understand the mechanism of enhanced cytotoxicity and apoptosis in IAB-1-treated versus huIFN-β protein-treated NC65 cells, we performed a cDNA macroarray. We identified eight genes among the 1185 human genes represented on the array, for which expression differed by ≥3-fold in NC65 cells treated by IAB-1 compared to NC65 cells treated with huIFN-β protein. Among these eight genes, *c-Myc* was of particular interest, because it is reported to be associated with proliferation and apoptosis (17-20). cDNA expression of c-Myc increased by 3.4-fold in NC65 cells treated with IAB-1 compared to huIFN-β protein. The level of c-Myc protein in whole cell lysates extracted 24 h after each treatment was examined by western blot analysis and

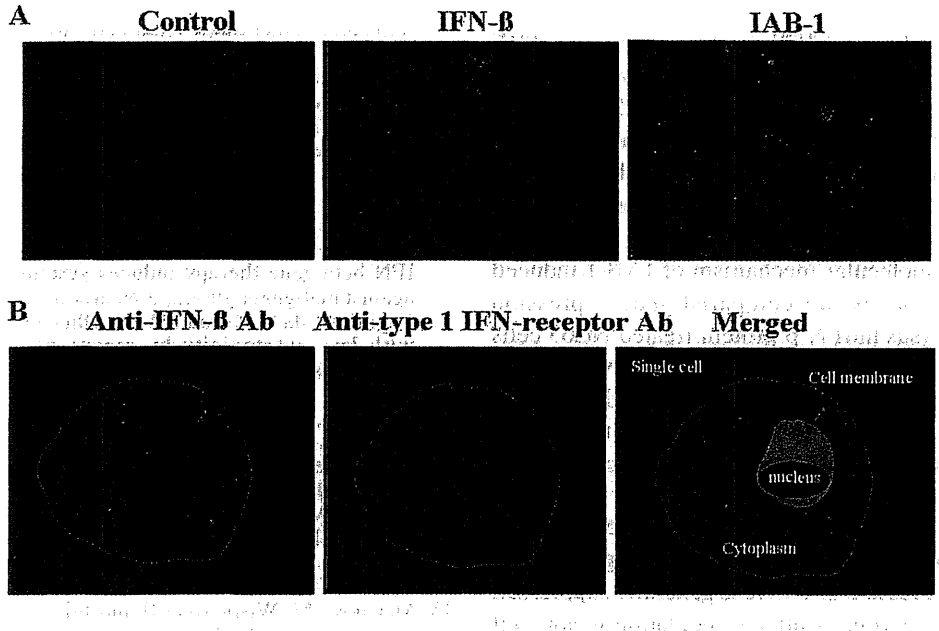

Figure 6. Subcellular localization of IFN-β protein and type 1 IFN-receptor. (A) Merged confocal microscopic images show the subcellular localization of IFN-β protein (green) and type 1 IFN-receptor (red) in NC65 cells by immunofluorescence. Cells were treated with PBS (control), 10000 IU/ml recombinant huIFN-β (IFN-β), or 0.1 μl/ml IAB-1 (IAB-1). (B) In NC65 cells treated with IAB-1, co-localization of huIFN-β protein (green) and type 1 IFN-receptor (red) was observed in the cytoplasm. In the merged image, superimposed white dotted lines delineate the cell membrane, and the gray area demarcates the nucleus.

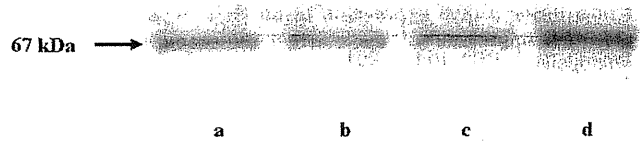

Figure 7. Western blot analysis of c-Myc expression. The relative expression levels of c-Myc protein were determined by western blot analysis using 20 μg whole lysate extracted from NC65 cells after treatment with (a) PBS (control), (b) 0.1 μl/ml of empty liposome (5.0 nmol lipid/ml), (c) 10000 IU/ml recombinant huIFN-β, or (d) 0.1 μl/ml of IAB-1 (5.0 nmol lipid with 0.1 μg plasmid DNA/ml). Cell lysates were separated on 10% polyacrylamide gels, and c-Myc protein (67 kDa) was detected with an anti-c-Myc antibody. Relative expression levels of c-Myc protein were quantified as follows: (a) 1.00, (b) 0.91, (c) 0.93, and (d) 1.91.

was found to be 2.1-fold higher in NC65 cells treated with IAB-1 compared to those treated with huIFN-β protein (Fig. 7).

Discussion

We previously reported that IAB-1 causes significant cytotoxicity against human RCC cells and that apoptosis was induced by IAB-1, but not by recombinant huIFN-β protein (9). However, the molecular mechanisms by which IAB-1, but not recombinant huIFN-β protein, induced apoptosis in the human RCC cell line NC65 were unclear. In this study, we examined the type 1 IFN signal transduction pathway in NC65 cells treated with IAB-1 and compared it to that in NC65 cells treated with recombinant huIFN-β protein. We first examined the status of extracellular signals induced by IAB-1 and huIFN-β protein. Neutralizing anti-huIFN-β antibodies decreased cytotoxicity in NC65 cells exogenously applied with huIFN-β protein, but not in NC65 cells transfected with IAB-1. This suggests that the IFN-β secreted from IAB-1-treated NC65 cells did not contribute to the enhanced cytotoxic and apoptotic effects. Furthermore, transwell experiments suggested that IAB-1 did not induce secretion of other molecules that may have contributed to increased cytotoxicity. Assessing downstream effects of the type 1 IFN signal transduction pathway, luciferase reporter assays indicated that ISRE activity was substantially enhanced by IAB-1.

To elucidate the molecular changes responsible for this increased activity, we examined the expression of ISGF3, which propagates signals triggered by IFN-IFN-receptor associations at the cell membrane through the cytoplasm and into nucleus, activating the ISRE. We found increased expression of the components of ISGF3 (STAT1, STAT2, and p48) in NC65 cells treated with either huIFN-β protein or IAB-1, although their levels did not significantly differ between the two treatments. We speculate that the activation of ISGF3, including phosphorylation, translocation into the nucleus, and expression of co-activators, is more highly induced by IAB-1 compared to huIFN-β protein. However, the molecular mechanism by which only IAB-1, but not huIFN-β protein, activates ISGF3 to enhance ISRE activity is unclear.

It has been reported that transfection of Fas ligand into prostate cancer cells resistant to monoclonal antibody-induced apoptosis induces Fas-mediated apoptosis associated with intracellular Fas ligand expression (21). In addition, it was recently reported that adenovirus encoding *IFN-α* caused marked cell growth inhibition and apoptosis in bladder, prostate, and ovarian cancer cell lines, all of which were resistant to IFN-α protein, in association with the perinuclear expression of IFN-α protein (22). Therefore, we examined the subcellular localization of huIFN-β protein and type 1 IFN-receptor after the transduction of IAB-1 into NC65 cells. Immunofluorescence revealed the co-localization of huIFN-β protein and type 1 IFN-receptor. We postulate that intracellular expression of huIFN-β protein

by IAB-1 transduction into RCC cells leads to the association of huIFN-β protein with type 1 IFN-receptor, enhancing ISRE activity. Our findings, together with those of previous studies (22), suggest that the intracellular expression of IFN protein by way of gene transfer may induce cytotoxicity of cancer cells that are otherwise resistant to IFN protein. Our results highlight the potential clinical application of IAB-1 for gene therapy in RCC cases resistant to IFN.

To elucidate the molecular mechanism of IAB-1-induced cytotoxicity and apoptosis, we compared gene expression profiles of IAB-1- versus huIFN-β protein-treated NC65 cells by cDNA macroarray. The cDNA macroarray revealed that c-Myc mRNA expression increased by 3.4-fold in NC65 cells treated with IAB-1 compared to huIFN-β protein. Western blot analysis confirmed a 2-fold increase in c-Myc protein in the same cells. The *c-Myc* promoter contains four regulatory sequences that are similar to ISRE (23). IRLB has been shown to bind this sequence, and its molecular cloning has been reported (23). The expression of c-Myc is generally suppressed by IFNs (23-26), but its transcriptional regulation is not well understood (23).

Furthermore, c-Myc has been reported to induce apoptosis under certain conditions (17-20). Enhanced expression of c-Myc protein in NC65 cells might be related to IAB-1-induced apoptosis. Additional studies are needed to confirm whether this is the case. It is also possible that other molecules play a role in IAB-1-induced apoptosis. Detailed understanding of the molecular mechanism of *IFN* gene transduction-induced apoptosis in IFN-resistant RCC will help develop more powerful therapeutic modalities for RCC patients that are resistant to conventional immunotherapies.

Acknowledgements

This work was supported in part by a 2002 Grant-in-Aid from the Japanese Urological Association in Japan. We acknowledge the technical assistance of Ms. Yukako Morioka.

References

1. Rinehart JJ, Young D, Laforge J, Colborn D and Neidhart JA: Phase I/II trial of interferon-beta-serine in patients with renal cell carcinoma: immunological and biological effects. Cancer Res 47: 2481-2485, 1987.
2. Motzer RJ, Bacik J, Murphy BA, Russo P and Mazumdar M: Interferon-alfa as a comparative treatment for clinical trials of new therapies against advanced renal cell carcinoma. J Clin Oncol 20: 289-296, 2002.
3. Jonasch E and Haluska FG: Interferon in oncological practice: review of interferon biology, clinical applications, and toxicities. Oncologist 6: 34-55, 2001.
4. Vuky J and Motzer RJ: Cytokine therapy in renal cell cancer. Urol Oncol 5: 249-257, 2000.
5. Escudier B, Eisen T, Stadler WM, *et al*: Sorafenib in advanced clear-cell renal-cell carcinoma. N Engl J Med 356: 125-134, 2007.
6. Hudes G, Carducci M, Tomczak P, *et al*: Temsirolimus, interferon alfa, or both for advanced renal-cell carcinoma. N Engl J Med 356: 2271-2281, 2007.
7. Motzer RJ, Escudier B, Oudard S, *et al*: Efficacy of everolimus in advanced renal cell carcinoma: a double-blind, randomised, placebo-controlled phase III trial. Lancet 372: 449-456, 2008.
8. Motzer RJ, Hutson TE, Tomczak P, *et al*: Sunitinib versus interferon alfa in metastatic renal-cell carcinoma. N Engl J Med 356: 115-124, 2007.
9. Nakanishi H, Mizutani Y, Kawauchi A, *et al*: Significant antitumoral activity of cationic multilamellar liposomes containing human IFN-beta gene against human renal cell carcinoma. Clin Cancer Res 9: 1129-1135, 2003.
10. Hoehn W and Schroeder FH: Renal cell carcinoma: two new cell lines and a serially transplantable nude mouse tumor (NC 65). Preliminary report. Invest Urol 16: 106-112, 1978.
11. Natsume A, Tsujimura K, Mizuno M, Takahashi T and Yoshida J: IFN-beta gene therapy induces systemic antitumor immunity against malignant glioma. J Neurooncol 47: 117-124, 2000.
12. Yagi K, Noda H, Kurono M and Ohishi N: Efficient gene transfer with less cytotoxicity by means of cationic multilamellar liposomes. Biochem Biophys Res Commun 196: 1042-1048, 1993.
13. Yoshida J, Mizuno M and Yagi K: Efficient transfection of human interferon-beta gene to human glioma cells by means of cationic multilamellar liposomes coupled with a monoclonal antibody [corrected]. J Neurooncol 19: 269-274, 1994.
14. Mizuno M, Yoshida J, Sugita K, *et al*: Growth inhibition of glioma cells transfected with the human beta-interferon gene by liposomes coupled with a monoclonal antibody. Cancer Res 50: 7826-7829, 1990.
15. Matsuoka M, Wispriyono B and Igisu H: Increased cytotoxicity of cadmium in fibroblasts lacking c-fos. Biochem Pharmacol 59: 1573-1576, 2000.
16. Mizutani Y, Nakanishi H, Li YN, Sato N, Kawauchi A and Miki T: Enhanced sensitivity of bladder cancer cells to cisplatin mediated cytotoxicity and apoptosis in vitro and in vivo by the selective cyclooxygenase-2 inhibitor JTE-522. J Urol 172: 1474-1479, 2004.
17. Askew DS, Ashmun RA, Simmons BC and Cleveland JL: Constitutive c-myc expression in an IL-3-dependent myeloid cell line suppresses cell cycle arrest and accelerates apoptosis. Oncogene 6: 1915-1922, 1991.
18. Couillard M, Guillaume R, Tanji N, D'Agati V and Trudel M: c-myc-induced apoptosis in polycystic kidney disease is independent of FasL/Fas interaction. Cancer Res 62: 2210-2214, 2002.
19. Pelengaris S, Khan M and Evan GI: Suppression of Myc-induced apoptosis in beta cells exposes multiple oncogenic properties of Myc and triggers carcinogenic progression. Cell 109: 321-334, 2002.
20. Prendergast GC: Mechanisms of apoptosis by c-Myc. Oncogene 18: 2967-2987, 1999.
21. Hyer ML, Voelkel-Johnson C, Rubinchik S, Dong J and Norris JS: Intracellular Fas ligand expression causes Fas-mediated apoptosis in human prostate cancer cells resistant to monoclonal antibody-induced apoptosis. Mol Ther 2: 348-358, 2000.
22. Zhang X, Yang Z, Dong L, Papageorgiou A, McConkey DJ and Benedict WF: Adenoviral-mediated interferon alpha overcomes resistance to the interferon protein in various cancer types and has marked bystander effects. Cancer Gene Ther 14: 241-250, 2007.
23. Semova N, Kapanadze B, Corcoran M, Kutsenko A, Baranova A and Semov A: Molecular cloning, structural analysis, and expression of a human IRLB, MYC promoter-binding protein: new DENN domain-containing protein family emerges small star, filled. Genomics 82: 343-354, 2003.
24. Chatterjee D and Savarese TM: Posttranscriptional regulation of c-myc proto-oncogene expression and growth inhibition by recombinant human interferon-beta ser17 in a human colon carcinoma cell line. Cancer Chemother Pharmacol 30: 12-20, 1992.
25. Dani C, Mechti N, Piechaczyk M, Lebleu B, Jeanteur P and Blanchard JM: Increased rate of degradation of c-myc mRNA in interferon-treated Daudi cells. Proc Natl Acad Sci USA 82: 4896-4899, 1985.
26. Sarkar D, Park ES and Fisher PB: Defining the mechanism by which IFN-beta dowregulates c-myc expression in human melanoma cells: pivotal role for human polynucleotide phosphorylase (hPNPaseold-35). Cell Death Differ 13: 1541-1553, 2006.

The Prostate 72:1124–1132 (2012)

High Mobility Group Protein AT-Hook 1 (HMGA1) Is Associated With the Development of Androgen Independence in Prostate Cancer Cells

Ichiro Takeuchi,[1] Natsuki Takaha,[1,2]* Terukazu Nakamura,[1] Fumiya Hongo,[1] Kazuya Mikami,[1] Kazumi Kamoi,[1] Koji Okihara,[1] Akihiro Kawauchi,[1] and Tsuneharu Miki[1,2]

[1]*Department of Urology, Kyoto Prefectural University of Medicine, Kyoto, Japan*
[2]*Department of Translational Cancer Drug Development, Kyoto Prefectural University of Medicine, Kyoto, Japan*

BACKGROUND. We previously reported that the level of high mobility group protein AT-hook 1 (HMGA1) is low in androgen-dependent prostate cancer (PCa) cells (LNCaP), but is high in androgen-independent PCa cells (DU145 and PC-3) and that HMGA1 is a strong candidate gene playing a potential role in the progression of PCa. These findings have prompted us to evaluate the effect of HMGA1 on developing androgen independency, which is associated with the progression of PCa.

METHODS. Expression of HMGA1 in PCa cells and mouse tissues was examined by Western blot. In order to examine the effect of HMGA1 on cell growth under androgen-deprived condition, we transfected HMGA1 into LNCaP cells, and siRNA into both DU145 and PC-3 cells, respectively.

RESULTS. Androgen-deprivation induced an increase in the level of HMGA1 in LNCaP cells in vitro and in vivo, but did not in normal prostate tissue. Overexpression of HMGA1 maintained the cell growth of LNCaP under androgen-deprived condition. Furthermore, knockdown of HMGA1 suppressed the cell growth of DU145 and PC-3.

CONCLUSIONS. These data suggest that elevated expression of HMGA1 is associated with the transition of PCa cells from androgen-sensitive to androgen-independent growth and plays a role in the cell growth of androgen-independent PCa cells. *Prostate 72:1124–1132, 2012.* © 2011 Wiley Periodicals, Inc.

KEY WORDS: **androgen-independence; HMGA1; prostate cancer; androgen-deprivation; castration-resistant**

INTRODUCTION

Prostate cancer (PCa) is the leading cancer diagnosis and the second most common cause of cancer-related death in men in the United States [1]. Initially, the growth of PCa is dependent on androgen and can be effectively treated by androgen-deprivation therapy (ADT). However, ADT only achieves a temporary regression in many cases of PCa, as almost all tumors will eventually progress to refractory to ADT after 1–3 years of the treatment. The majority of the deaths from PCa result from metastatic castration-resistant PCa (CRPC). Understanding the mechanisms by which androgen-sensitive tumor cells lose androgen-dependence or otherwise acquire the ability to grow under androgen-deprived condition has therefore been an important objective in the quest for effective treatment of PCa. Recent advances identified several possible mechanisms and pathways involved in the development of androgen-independent PCa cells.

It is also important to identify which gene alterations induced by androgen-deprivation are involved in the development of androgen-independent PCa cells.

*Correspondence to: Dr. Natsuki Takaha, Departments of Urology and Translational Cancer Drug Development, Kawaramachi-Hirokoji, Kyoto 602-8566, Japan. E-mail: ntakaha@koto.kpu-m.ac.jp
Received 2 October 2011; Accepted 27 October 2011
DOI 10.1002/pros.22460
Published online 27 December 2011 in Wiley Online Library (wileyonlinelibrary.com).